

New Cement Nano-Spacer to Optimize Wellbore Cleaning

By

Fuad Bin Othman
12336

Dissertation submitted in partial fulfilment of the requirements for the
Bachelor of Engineering (Hons) Petroleum Engineering

SEPTEMBER 2011

Universiti Teknologi PETRONAS
Bandar Seri Iskandar
31750 Tronoh
Perak Darul Ridzuan

CERTIFICATION OF APPROVAL

New Cement Nano-Spacer to Optimize Wellbore Cleaning

By

Fuad Bin Othman
12336

A project dissertation submitted to the Petroleum Engineering Programme
Universiti Teknologi PETRONAS
In Partial Fulfilment of the requirement for the
Bachelor of Engineering (Hons) Petroleum Engineering

Approved

.....
(Dr Sonny Irawan)

Project Supervisor

UNIVERSITI TEKNOLOGI PETRONAS
TRONOH, PERAK
SEPTEMBER 2011

CERTIFICATION OF ORIGINALITY

This is to certify that I am responsible for the work submitted in this project, that the original work is my own except as specified in the references and acknowledgments and that the original work contained herein have not been undertaken or done by unspecified sources or persons.

.....
(Fuad Bin Othman)

Petroleum Engineering Department
Universiti Teknologi PETRONAS

ACKNOWLEDGEMENT

In the name of Allah, the Most Gracious, the Most Merciful. Praise to Him the Almighty that His blessing and guidance in giving me strength, courage, patience, and perseverance to endure this Final Year Project.

First of all, I would like to convey my highest gratitude to my Final Year Project Supervisor, Dr Sonny Irawan for her continuous support, knowledge, and words that kept me moving to complete this research project.

I also would like to thanks all the lab technologist in Petroleum Engineering Department for their help in formulate my Nano-Spacer especially Amirul and Reduan.

And not to forget, a post-graduate student who's have been assisting me in carrying out this research; Ms Rasyada Ahmad, for her guidance and always been a great help in making this final year project a success.

Finally, thanks to my very own Universiti Teknologi PETRONAS, for the facilities, laboratories and consumables given to me.

ABSTRACT

New nano-spacer is a formulation to create and promote better cement bonding. This is due to the current spacer used in oil and gas industry currently doesn't remove all mud attached to the casing thus promoting poor cement bonding between casing and cement.

Efficient mud removal, filter cake removal and formation clean-up are critically required for well cementing, production and injection wells drilled with non-aqueous mud. Conventional surfactant clean-up system requires a turbulent flow and large volume to solubilise residue efficiently. Unsuitable surfactant system may cause emulsion blockage and oil-contamination in the completion brine, which consequently leads to a reduction in oil production rate. A new potential method to improve and overcome these problems with higher efficiency to remove non-aqueous mud by using the nano-fluid technology.

This technology has the ability to reduce the oil-water interfacial tension of Oil Based Mud down to 2 mN/m. Not to forget with a small amount (0.1 wt%) of nano-particles being dispersed into water, the ability of the nano-fluid can increase up to 80% cleaning compared to the current cement spacer technology which only able to clean for 40%.

TABLE OF CONTENTS

CERTIFICATION OF APPROVAL	ii
CERTIFICATION OF ORIGINALITY	iii
ACKNOWLEDGEMENT.....	iv
ABSTRACT.....	v
TABLE OF CONTENTS	vi
LIST OF FIGURES	viii
LIST OF TABLES	x
CHAPTER 1: INTRODUCTION.....	1
1.1 Background of Study.....	1
1.2 Problem Statement	3
1.2.1 Problem Identification	3
1.2.2 Significant of the Project	3
1.3 Objectives.....	4
1.4 Scope of Study	5
CHAPTER 2: LITERATURE REVIEW	6
2.1 Casing Cementation	6
2.2 Spacer.....	9
2.3 Bentonite as Weighting Agent	11
2.4 Xanthan Gum as Viscosifier	12
2.5 Surfactant as IFT Reducing Agent.....	14
2.6 Wellbore Cleaning.....	16

CHAPTER 3: METHODOLOGY	18
3.1 Project Workflow	18
3.2 Procedures	20
3.2.1 Nano-fluid Preparation.....	20
3.2.1 Nano-fluid Preparation Metallic Grid Test.	22
3.2.3 Interfacial Tension Test (IFT) Spinning Drop.	23
3.3 Gantt chart	24
CHAPTER 4: RESULTS AND DISCUSSION	25
4.1 Nano-Fluid Preparation.	25
4.2 Metallic Grid Test	34
4.3 Interfacial Tension Test (IFT).	39
CHAPTER 5: CONCLUSION AND RECOMMENDATION	42
5.1 Conclusion.....	42
5.2 Recommendations	42
REFERENCES.....	43
APPENDICES	45

LIST OF FIGURES

FIGURE 1: Spacer used in two stage cementing operation (Ref: Wikipedia.com)	10
FIGURE 2: Bentonite (Ref: Wikipedia.com)	11
FIGURE 3: Structural formula of Xanthan Gum (Ref: Becker and Vorholter (2009) "Xanthan Gum Biosynthesis")	13
FIGURE 4: Surfactant Molecule [Rosen MJ (2012)].....	14
FIGURE 5: Surfactant at Hydrophilic/Hydrophobic medium interface [Rosen MJ (2012)] .	14
FIGURE 6: Surfactant Micelle[Rosen MJ (2012)].....	15
FIGURE 7: Effect of surfactant concentration on surface tension & micelle formation [Rosen MJ (2012)]	15
FIGURE 8A: XRD Pattern for ZnO using Ethylene Glycol (EG) nanoparticles for standard ZnO and annealed at temperature 300°C and 400°C	26
FIGURE 8B: XRD Pattern for ZnO using Nitric Acid (HNO ₃) nanoparticles for standard ZnO and annealed at temperature 300°C and 400°C	26
FIGURE 9A: FESEM image For ZnO by using Ethylene Glycol nanoparticles annealed at temperature 300°C	28
FIGURE 9B: FESEM image For ZnO by using Ethylene Glycol nanoparticles annealed at temperature 400°C	29
FIGURE 9C: FESEM image For ZnO by using Ethylene Glycol nanoparticles annealed at temperature 500°C	29
FIGURE 10A: FESEM image For ZnO by using Nitric Acid nanoparticles annealed at temperature 300°C	30
FIGURE 10B: FESEM image For ZnO by using Nitric Acid nanoparticles annealed at temperature 400°C	30

FIGURE 10C: FESEM image For ZnO by using Nitric Acid nanoparticles annealed at temperature 500°C	31
FIGURE 11A: Graph for Nano-fluid Metallic Grid Test.	37
FIGURE 11B: Graph for Nano-fluid by using Ethylene Glycol as a dispersed medium Metallic Grid Test.	37
FIGURE 11C: Graph for Conventional Spacer Metallic Grid Test.	38
FIGURE 12A: Snapshot image from SVT20 Tensiometer during the measurement shows the drop size at rotation 1,000 rpm	40
FIGURE 12B: Snapshot image from SVT20 Tensiometer during the measurement shows the drop size at rotation 5,000 rpm	40
FIGURE 13: Molecular structure of sodium dodecyl sulfate, showing the polar head and non-polar tail [9] (Ref: P. Mukerjee "Critical Micelle Concentration of Aqueous Surfactant Systems")	41

LIST OF TABLES

TABLE 1: Cement Slurry Specification (Ref: Lawrence Webber. (2004), “Global Best Practice for Cementing”)	7
TABLE 3B: Gantt chart for FYP2	24
TABLE 4: Comparative values of crystal planes, d-spacing, lattice parameter, structure and crystallite size of ZnO nanoparticles annealed at various temperatures	27
TABLE 5: Elemental distribution analysis of zinc oxide nanoparticles annealed at various temperatures.....	32
TABLE 6A: Table Results for Metallic Grid Test.....	34
TABLE 6B: Table Results for Metallic Grid Test.....	35
TABLE 7: Table Results for Contact Angle Test.....	39

CHAPTER 1: INTRODUCTION

1.1 Background of Study

Cementing operation is an important aspect during exploration and production. This is because it creates a solid boundary between the casing and formation which acts as a formation isolator. Cementing operation plays a critical role in the drilling process of a well and mud displacement is very important for achieving a good cement bond to maintain well integrity and subsequent production performance.

Pill used to separate the cement slurry from the drilling mud are termed “SPACERS”. Spacers are designed in a manner such that their densities, gel strengths and viscosity are more than that of the drilling fluid and less than that of the cement slurry. In cement job the corrected application of the hierarchies of density and rheology during the OBM displacement is necessary, but isn't sufficient to guarantee a good cleaning of the casing-bore and reverse wettability; these properties are necessary to obtain good adhesion of slurry to casing/formation. In order to avoid cement job failure, a number of spacer has been used with different degree of success. Solvent spacers are also been considered (Morris et al., 1973) and Nowadays innovative spacers have been developed looking for more effective formulations.

Cement Nano-Spacer is a newly formulate mixture in a nano-emulsion form. It is called “Nano-Spacer” because of its droplet size properties of internal phase is less than 500 nm. Due to its small dimensions they have high surface area and show very extraordinary properties. Due to the presence of the surfactant mixture used to prepare the nano-spacer, the solvent in water nano-spacer combined the high efficiency of the small dimensions of solvent to a low interfacial tension. The water solvent nano-spacer can be used to separate cements and mud where it would allowed optimizing the cleaning of the casing during the cement job with a high improvement of the performance of the spacers currently in use. The procedure is based on the high efficiency system with reduced chemical dosage where it would also results in a substantial cleaning optimization where it could promote better cement bonding during cementing/completion process.

The objectives of this study are to formulate nano-fluid through continuously stirring method directly with a selected solvent as its internal phase. The efficiency is evaluated throughout certain test; Metallic Grid test and Contact Angle Test. At the end of the experiment we found out that using the nano-fluid technology we are able to improve the cleaning efficiency 80% more than the conventional spacer.

1.2 Problem Statement

1.2.1 Problem Identification

In the industry, the spacer used during the completion and drilling operation doesn't provide the optimization of casing cleaning. Due to this problem, weak cement bonding between the casing and the cement occurred.

In addition to that, weak cement bonding will create major problem in formation isolation in the wellbore. Not to forget this could cause major production problem after some time. With the help of nano-particle sized of Zinc Oxide, we could improve the cleaning efficiency of the current spacer thus indirectly promotes a better cement bonding to avoid any major problems in the future during production.

1.2.2 Significant of the Project

In Malaysia and many other countries, most mature reservoirs are already water flooded, or are presently being subjected to secondary and tertiary recovery processes. In Malaysian oil reservoirs, only about 36.8% of original oil in place (OOIP) is produced through the entire life of mature reservoirs that have been developed under conventional methods (Hamdan et al., 2005). A significant amount of hydrocarbon would not be recovered utilizing the current production strategies, and that has motivated Malaysia to attempt Enhanced Oil recovery (EOR). Recognizing the potential of EOR in the fields, the national oil company (PETRONAS) endorsed a comprehensive EOR screening in year. The screening study on seventy two reservoirs has identified almost a billion barrels of additional reserves can be achieved through EOR (Samsuddin et al., 2005). The Chemical Enhanced Oil Recovery (CEOR) was identified as one of the key EOR processes that have good potential for field implementation to increase ultimate recovery in Malaysian oil fields (Othman et al., 2007). These include surfactant flooding.

Therefore, in this project, the author examined the performance and effectiveness of cleaning by using a small amount of nano-particles (1 wt% of ZnO) in the drilling fluid to act as a spacer during cementing operation. It is also important in cementing operation that no problems occurred during production after using the nano-spacer as cleaning and scrubbing agent.

1.3 Objectives

This research is carried out to study the effectiveness of adding nano-particles into the spacer to enhanced wellbore cleaning.

- a. To formulate new cement nano-spacer by using 1 wt% of Nano-particle size Zinc Oxide and disperse them into an aqueous solution by using FESEM, EDX and XRD to check the characteristics of the nano-particles.

- b. To determine the cleaning efficiency of the new cement nano-spacer through Metallic Grid Test where it uses Viscometer and Weighing machine for obtaining the % Mud Removal and IFT test via spinning drop to check the reduction of Interfacial Tension after using the nano-spacer formulated earlier.

1.4 Scope of Study

The study will utilize the usage of nano-sized Zinc Oxide that used in Enhance Oil Recovery into the application of Spacer (drilling fluids).

- i. Investigate the use of spacer during cementing operation.
- ii. Production of nano-fluid by using Sol-gel method.
- iii. Characterize the Nano-particles obtained.
- iv. Run the optimization test towards the emulsion fluid; Metallic Grid Test and IFT test.

CHAPTER 2: LITERATURE REVIEW

2.1 Casing Cementation

During Petroleum Exploration, Production, Drilling or even Abandonment, cementing a well is the procedure of developing and pumping cement into place in a wellbore before further operation can be done.

Used for a number of different reasons, cementing protects and seals the wellbore. Most commonly, cementing is used to permanently shut off water penetration into the well. Part of the completion process of a prospective production well, cementing can be used to seal the annulus after a casing string has been run in a wellbore. Additionally, cementing is used to seal a lost circulation zone, or an area where there is a reduction or absence of flow within the well. In directional drilling, cementing is used to plug an existing well, in order to run a directional well from that point. Also, cementing is used to plug a well to abandon it.

Cementing is performed when the cement slurry is deployed into the well via pumps, displacing the drilling fluids still located within the well, and replacing them with cement. The cement slurry flows to the bottom of the wellbore through the casing, which will eventually be the pipe through which the hydrocarbons flow to the surface. From there it fills in the space between the casing and the actual wellbore, and hardens. This creates a seal so that outside materials cannot enter the well flow, as well as permanently positions the casing in place.

Before cementing operation is held, a slurry design must be made. This design addresses a broad assortment of well conditions and well control parameters. In order to get the maximum performance of slurry, there are 7 rules and strategy to hold on to;

Cement Slurry Specifications

Slurry Properties	Conductor and Surface Casings	Intermediate Casings and Drilling Liners	Production Casings and Liners	Deep Production Liners and for Gas Control
Density	+ 1 ppg > drilling fluid density			
	< Equivalent Circulating Density (ECD) to fracture formation			
Thickening Time	Job time plus at least one hour for safety factor			
	For production casings or for gas control, the TT chart should display a right angle set (transition from 40 to 100 Bc in less than 15 minutes)			
Free Water	≤ 1.0%	≤ 0.5 %	0 %	0 %
Fluid Loss	NA	≤ 250	≤ 100	≤ 50
Rheol. (PV)	≤ 150	≤ 150	≤ 100	≤ 100
Rheol. (YP)	≤ 50	≤ 40	≤ 25	≤ 20
Comp. Strength WOC (hr to 500 psi)	≤ 12	≤ 8	≤ 8	≤ 8
24-hr Comp. Strength (psi)	1,000	2,000	2,000	2,000

Table 1: Cement Slurry Specification (Ref: Lawrence Webber. (2004), “Global Best Practice for Cementing”)

First is about the density. Cement slurry density must be within range to maintain well control. If the condition of the hole allows, cement slurry density should be a minimum of 1.0 ppg greater than drilling fluid weight and 0.5 ppg greater than the spacer weight.

Next, the thickening time should be considered. The pump time should include the estimated job time plus a safety factor. The safety factor must be based on wellbore parameters, operational objectives and limitation, and the accuracy of expected temperature to which the cement slurry will be exposed during the cementing process as compared to the laboratory testing conditions.

Not to forget, the mixability of the mixture also should be considered. Cement must be easy to mix at the cementing unit in order to achieve density control at a mixing rate that allows cement slurry placement within available pump time.

Next is the Rheology of the slurry. The cement slurry must be pump-able, and the cement slurry rheological properties must allow effective placement, with a plastic viscosity; PV, and yield point; YP, as low as possible, but higher than that of spacer or drilling fluid.

Fluid loss control is also a major aspect in the design. Design fluid lost control to specification. Excessive loss of fluid from the cement slurry has negative impact on other slurry properties.

Moreover, the compressive strength of the cement is also critical. The goal is to achieve rapid compressive strength development after placement. The minimum requirement is a “Waiting on Cement”; WOC, time (time to achieve 500 psi) of less than 12 hours and 24 hours strength greater than 1,000 psi.

The stability of the cement should be considered in terms of free fluid an settling. Cement slurry must remain stable (free water within specification and no significant settling or separation) while fluid. Design and test for given hole conditions, i.e. for direction well test at appropriate angle.

2.2 Spacer

Spacer is a viscous fluid or mixture which is used to help the removal of drilling fluids before a primary cementing operation. They are an effective displacement aids because they separate unlike fluids such as cement and drilling fluid, and enhance the removal of gelled drilling fluid, allowing a better cement bond. Spacer can be designed to serve various needs. For instance, a weighted spacer can help with well control and reactive spacers can provide increase in drilling fluid-removal benefits. Compatibility of the drilling fluid/spacer as well as the compatibility of the spacer/cement slurry is of prime importance.

Parameters governing a spacer's effectiveness include flow rate, contact time, and fluid properties. To achieve maximum drilling fluid displacement, we can take into account these few properties;

Firstly is the density. The spacer density should be set at 0.5 to 1.0 ppg above the drilling fluid weight and at least 0.5 ppg less than the cement slurry density. In the situation that require the difference between cement weight and drilling fluid weight to be less than 1.0 ppg, design the spacer density to be mid-way between the two densities.

Next is the contact time. These spacers also need to provide a contact time and volume of spacer that will provide optimum amount of drilling fluid removal. Typically 8 to 10 minutes contact time or 1,000 feet of annular space are adequate.

Moving along, the rheology of the spacer should also be considered. Spacer design Rheology is important as this will provide turbulent flow where hole geometry allows. Turbulent flow of spacer is required on all liner jobs.

The compatibility of the spacer is also a must. Spacer must be fully compatible with drilling fluid and cement. Contact with drilling fluid must not result in flocculation, settling, or excessive rheology. Contact with cement must not decrease pump time.

Next is the stability of the mixture. Spacer must remain stable with no excessive settling or separation. For all liner and tieback jobs, the spacer must be tested by "hot-rolling" at circulating temperature.

Last but not least, is the wettability of the mixture. When oil-based or synthetic-based drilling fluid is in the hole, the spacer must also be capable of converting the pipe and hole to a “water wet” condition.

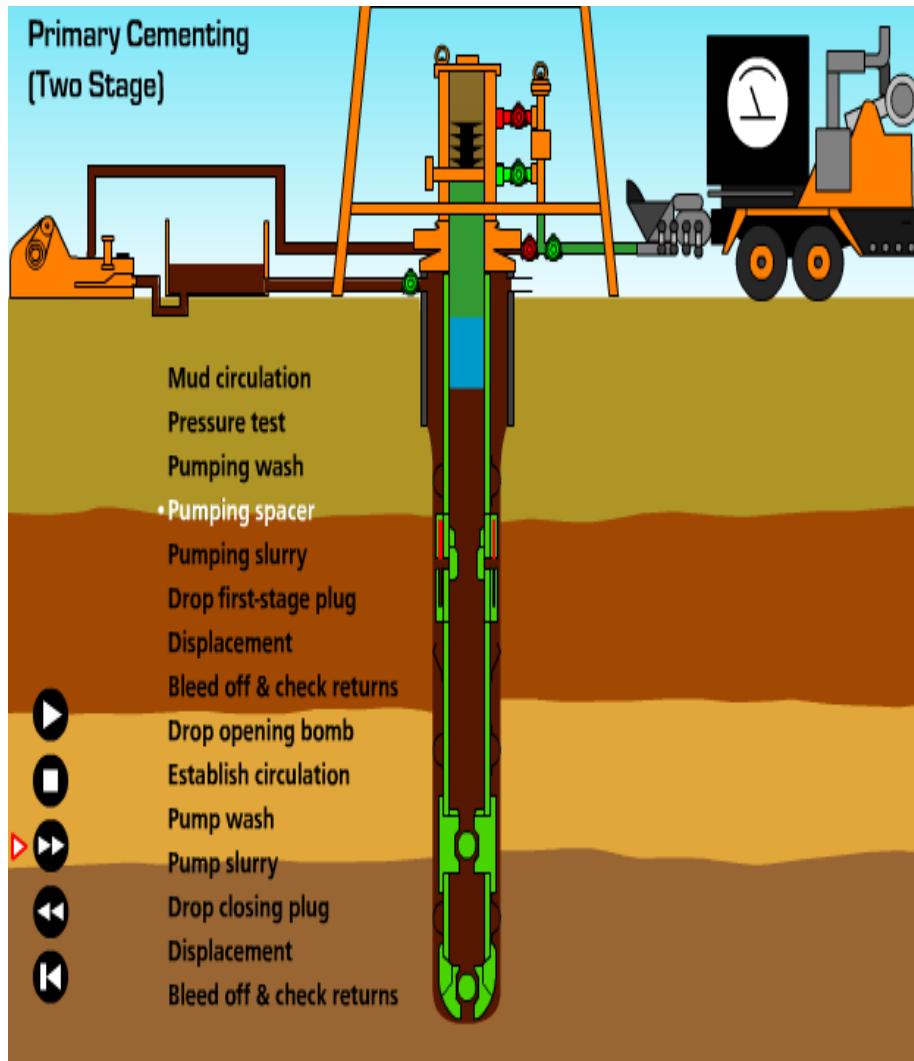


FIGURE 1: Spacer used in two stage cementing operation (Ref: Wikipedia.com)

2.3 Bentonite as Weighting Agent

Bentonite is an absorbent aluminium phyllosilicate, essentially impure clay consisting mostly of montmorillonite. There are different types of Bentonite, each named after the respective dominant element, such as potassium (K), sodium (Na), calcium (Ca), and aluminium (Al). Experts debate a number of nomenclatorial problems with the classification of Bentonite clays. Bentonite usually forms from weathering of volcanic ash, most often in the presence of water. However, the term Bentonite, as well as similar clay called tonstein, has been used for clay beds of uncertain origin. For industrial purpose, two main classes of Bentonite exist: sodium and calcium Bentonite. In stratigraphy and tephrochronology, completely devitrified (weathered volcanic glass) ash-fall beds are commonly referred to as K-Bentonites when dominant clay species is illite. Other common clay species, and sometimes dominant, are montmorillonite and kaolinite. Kaolinite-dominated clays are commonly referred to as tonsteins and are typically associated with coal.

Much of bentonite's usefulness in the drilling and geotechnical engineering industry comes from its unique rheological properties. Relatively small quantities of Bentonite suspended in water form a viscous, shear thinning material. Most often, Bentonite suspensions are also thixotropic, although rare cases of rheopectic behaviour have also been reported. At high enough concentration (60g of Bentonite per litre of suspension), Bentonite suspension begin to take on the characteristics of a gel (a fluid with a minimum yield strength required to make it move). For these reason it is a common component of drilling mud used a curtail drilling fluid invasion by its propensity for aiding in the formation of mud cake.



FIGURE 2: Bentonite (Ref: Wikipedia.com)

2.4 Xanthan Gum as Viscosifier

Xanthan Gum is a biopolymer; polysaccharide. This polymer is originally derived from the strain of bacteria used during the fermentation process, *Xanthomonas Campestris*. Sometimes you may hear the same bacterium is responsible for causing black rot to form on broccoli, cauliflower and other leafy vegetables. The bacteria form a slimy substance which acts as a natural stabilizer or thickener. It was developed when the United States Department of Agriculture ran a number of experiments involving bacteria and various sugars to develop a new thickening agent similar to corn starch or guar gum.

One of the most remarkable properties of Xanthan gum is its ability to produce a large increase in the viscosity of a liquid by adding a very small quantity of gum, on the order of one percent. In most foods, it is used at 0.5%, and can be used in lower concentrations. The viscosity of Xanthan gum solutions decreases with higher shear rates; this is called shear thinning or pseudo plasticity. This means that a product subjected to shear, whether from mixing, shaking or even chewing, will thin out, but once the shear forces are removed, the food will thicken back up. A practical use would be in salad dressing: the Xanthan gum makes it thick enough at rest in the bottle to keep the mixture fairly homogeneous, but the shear forces generated by shaking and pouring thins it, so it can be easily poured. When it exits the bottle, the shear forces are removed and it thickens back up, so it clings to the salad. Unlike other gums, it is very stable under a wide range of temperatures and pHs.

In foods, Xanthan gum is most often found in salad dressings and sauces. It helps to prevent oil separation by stabilizing the emulsion, although it is not an emulsifier. Xanthan gum also helps suspend solid particles, such as spices. Also used in frozen foods and beverages, Xanthan gum helps create the pleasant texture in many ice creams, along with guar gum and locust bean gum. Toothpaste often contains Xanthan gum, where it serves as a binder to keep the product uniform. Xanthan gum (when sometimes not made from wheat—see below for gluten-free allergy information) is also used in gluten-free baking. Since the gluten found in wheat must be omitted, Xanthan gum is used to give the dough or batter a “stickiness” that would otherwise be achieved with the gluten. Xanthan gum also helps thicken commercial egg substitutes made from egg whites, to replace the fat and emulsifiers found in yolks. It is also a preferred method of thickening liquids for those with swallowing

disorders, since it does not change the colour or flavour of foods or beverages at typical use levels.

In cosmetics, Xanthan gum is used to prepare water gels, usually in conjunction with Bentonite clays. It is also used in oil-in-water emulsions to help stabilise the oil droplets against coalescence. It has some skin hydrating properties. Xanthan gum is a common ingredient in fake blood recipes, and in gunged/slime.

In the oil industry, Xanthan gum is used in large quantities, usually to thicken drilling mud. These fluids serve to carry the solids cut by the drilling bit back to the surface. Xanthan gum provides great “low end” rheology. When the circulation stops, the solids still remain suspended in the drilling fluid. The widespread use of horizontal drilling and the demand for good control of drilled solids has led to its expanded use. It has also been added to concrete poured underwater, to increase its viscosity and prevent washout.

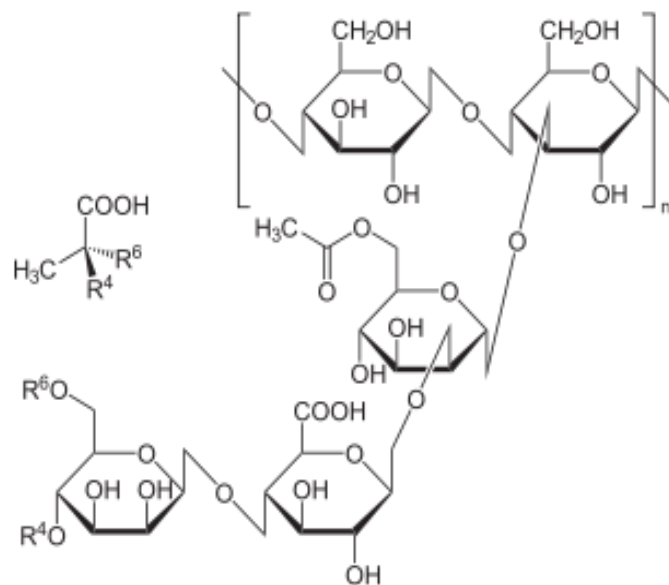


FIGURE 3: Structural formula of Xanthan Gum (Ref: Becker and Vorholter (2009) "Xanthan Gum Biosynthesis")

2.5 Surfactant as IFT Reducing Agent

Surfactant is an organic molecule that adsorbs at the gas-in-liquid, liquid-in-liquid or solid-in-liquid interface and lowers the surface/interfacial tension. It consists of two well-defined moieties, one is the water-soluble which is called the hydrophilic part, and the other is oil-soluble which is called the hydrophobic part.

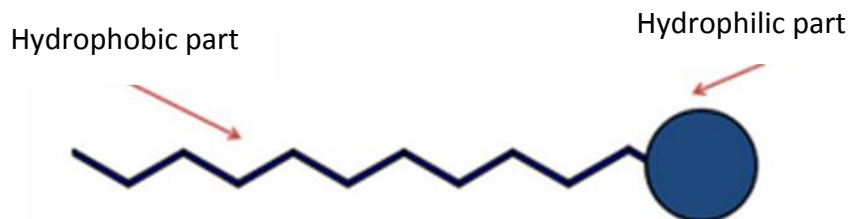


FIGURE 4: Surfactant Molecule [Rosen MJ (2012)]

At the absorption part, the hydrophilic part of the surfactant will partition in aqueous medium, whereas, the hydrophobic part will partition in non-aqueous medium.

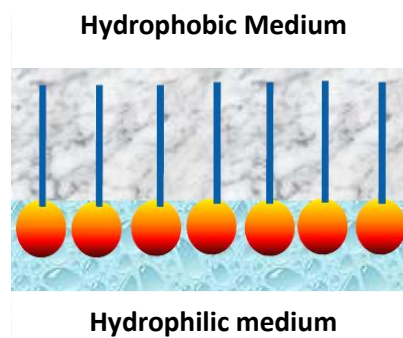


FIGURE 5: Surfactant at Hydrophilic/Hydrophobic medium interface [Rosen MJ (2012)]

There are two unbalance forces act onto the molecules: one is entropy driven, which is lead by attractive hydrophobic forces or Van der Waar's forces among the hydrophobic tails group; and one is enthalpy driven, which is dominated by the electrostatic repulsive forces at the hydrophilic head group. To minimize the Gibbs free energy, surfactant molecules tend to self-coagulate themselves and form a 3-D molecular cluster called "micelle". Inside these micelles are the hydrophobic region that promote the partition of the oily hydrocarbons; which are separate by a pseudo-membrane that contributed by the hydrophilic head groups.

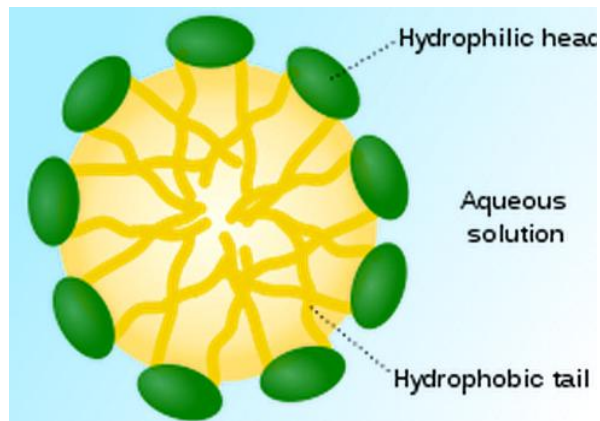


FIGURE 6: Surfactant Micelle[Rosen MJ (2012)]

Surfactants molecules tend to make partition at the air-water interface, thus displacing water molecules. This will then results in the reduction of Interfacial Tension. The linear relation of the surface tension-surfactant concentration can be found as the concentration of surfactant increase. At some point where the surface tension reaching its minimum, there is no further reduction in surface tension upon addition surfactants. This concentration is defined as the critical micelle concentration (CMC) of the surfactant. At the CMC, additional of surfactant molecules will lead to the creation of the new micelles since the air-water surface already being saturated by surfactants.

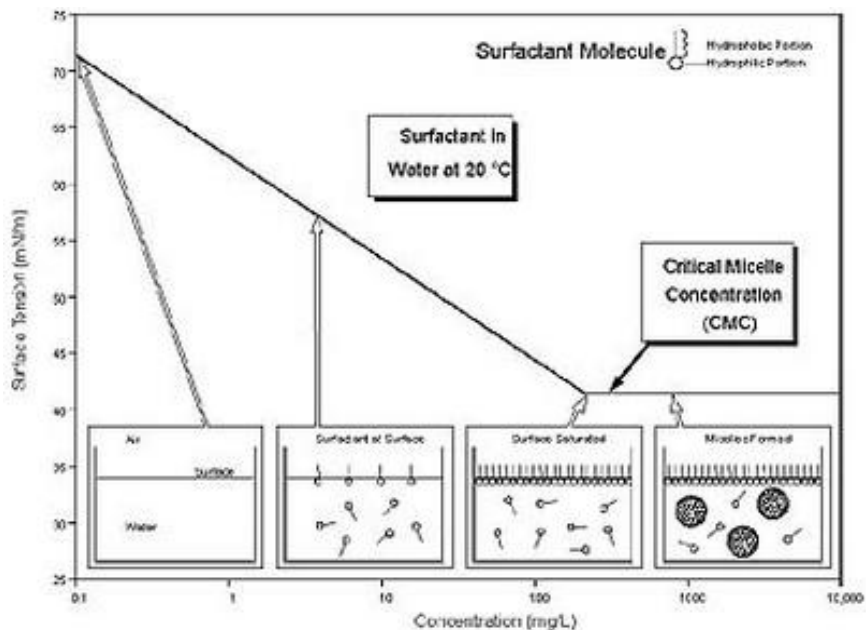


FIGURE 7: Effect of surfactant concentration on surface tension & micelle formation [Rosen MJ (2012)]

2.6 Wellbore Cleaning

During the exploration for oil and gas, boreholes are drilled deep into the earth surface. These holes are lined with casing. This casing is usually composed of heavy steel pipes, and cement is forced down the casing and up the annulus between the outer wall of the casing and the borehole wall. The cement is then forced to the bottom of the casing with a displacement fluid, typically drilling mud. Normally, a variety of drilling muds can be used for drilling. The drilling muds are generally water-based containing solids or non-aqueous based muds can be weighted with weighting material such as barite or non-weighted. The main function for drilling mud is to provide hydrostatic pressure to prevent formation fluids from entering into the wellbore, keeping the drill bit cool, cleaning during drilling, carrying out drill cutting and suspending the drill cuttings. The drilling fluids used for a particular job is selected to avoid formation damage and to limit corrosion.

Moreover, viscosifiers are also added to improve the mud rheology, bridging agents, such as calcium carbonate and Xanthan gum, are added to enhance the filter cake formation to prevent the invasion of fluids into the formation.

Filter cake formation has to be well controlled in order to prevent some catastrophic events. If the thickness of filter cake is too thin, there will be an imbalance pressure across the filter cakes and excessive fluids exchange may occur across the wall of the wellbore. If the thickness is too much, then it may lead to tight hole condition, poor log quality, stuck pipe, lost circulation and formation damage. These issues consequently induce in a major problem of dramatic reduction in the oil production rate and wellbore stability.

In general, there are two types of displacement spacers. First is the non-aqueous-based and second is the aqueous-based spacer. These are used typically in wellbore cleaning during cementing operation. Non-aqueous-based spacers are normally toxic and not environmentally friendly. Well surface after treatment is not water-wet and thus it still requires a further treatment with surfactant solution to alter the wettability of the wellbore surface and formation into water-wet.

However, in aqueous-based spacers, surfactant or surfactant-in-solvent mixtures have been used in displacement spacer for removing the non-aqueous-based mud and filter cake in the well bore. Surfactants are also used to change the wettability of well wall surface or

formation rocks surface to water-wet. However, this treatment requires a turbulent flow and large quantity of surfactants to solubilise the residue in a much more efficient way.

Usually surfactant solutions are only able to solubilise small quantity of oily hydrocarbons and usually need a turbulent flow or mechanical shear to remove those hydrocarbons.

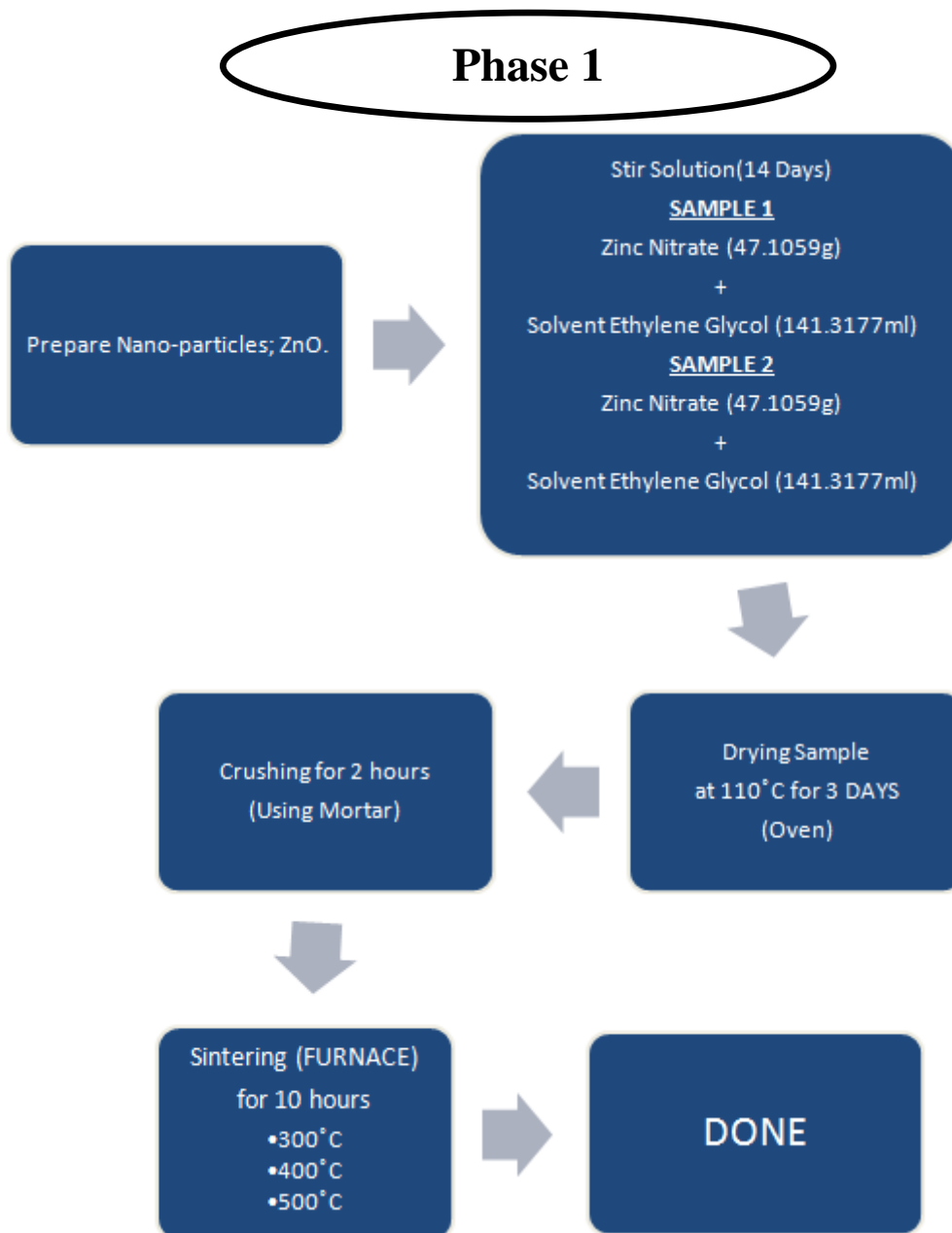
In Nano-emulsion technology, the oily hydrocarbons tend to partition within the nano-micellar structure spontaneously due to its ultra-low interfacial tension (IFT). This has been described by Gibbs free energy equation:

$$dG = \gamma dA - TdS \quad \text{Eq. (1)}$$

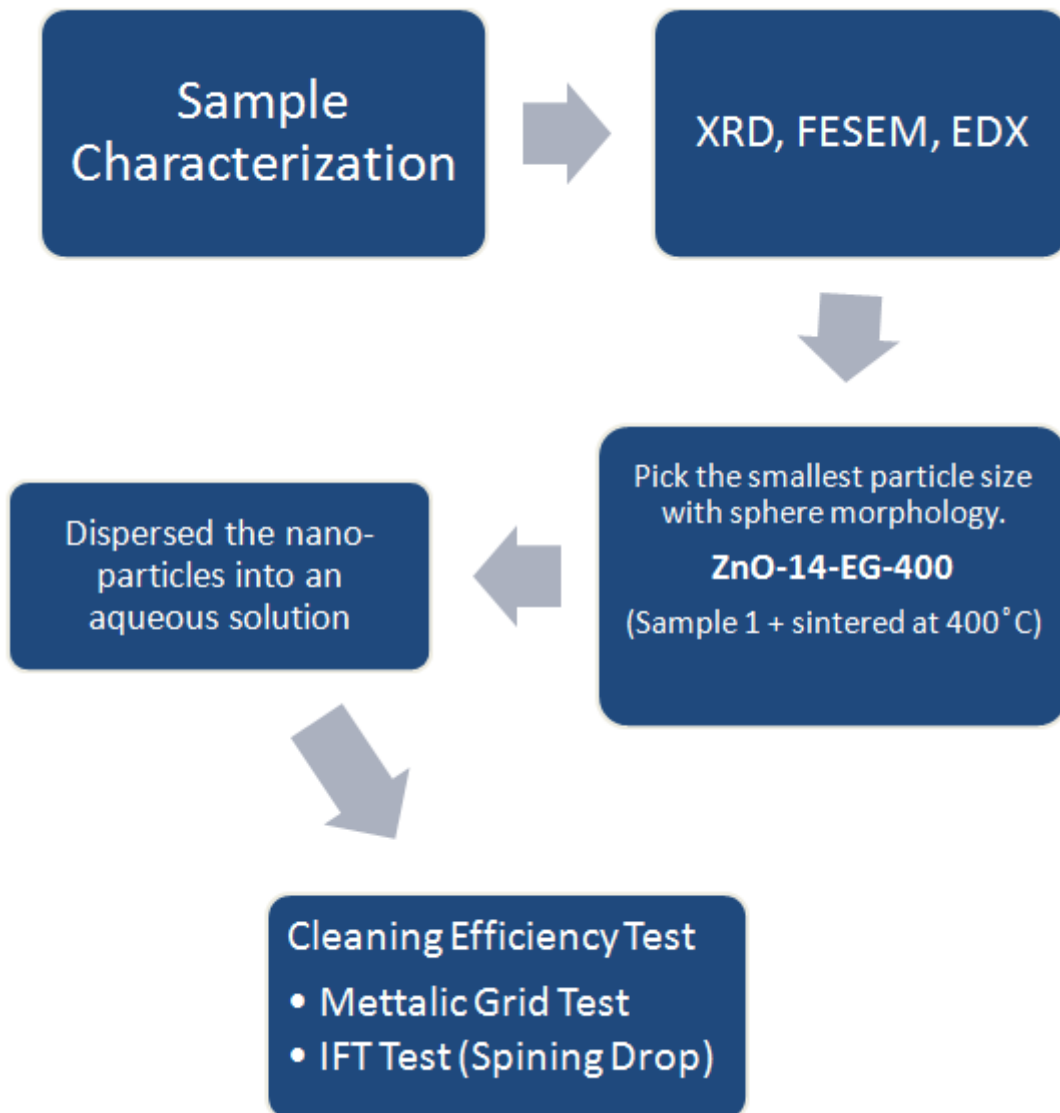
Where; G: Gibbs free energy, γ : interfacial tension, A: Surface area, T: Temperature, S: Entropy

CHAPTER 3: METHODOLOGY

3.1 Project Workflow



Phase 2



3.2 Procedures

3.2.1 Nano-fluid Preparation.

At this section, the author will be describing about the preparation of the nano particles and the methods and equipments used to create and characterize in order to obtain the nano-spacer before carrying out the cleaning efficiency test.

3.2.1.1 Preparation of ZnO by Sol Gel Method

Metal oxides, namely zinc oxide was prepared by dissolving the metal nitrates in acidic solvent. In the preparation of zinc oxide, zinc nitrate hexahydrate, $Zn(NO_3)_2 \cdot 6H_2O$ of 98.0% purity was purchased from R&M Chemicals serves as a precursor and dissolved in 100% nitric acid, HNO_3 and Ethylene Glycol, 1,2-ethanediol. The reason we're using two different solvent to dissolve the precursor is because the aim of the preparation of ZnO is to obtain different nano-sized crystallized shape of ZnO. The target shape for this preparation is a sphere shape of nanoparticle size of ZnO. The solution then was stirred continuously in 14 days to ensure homogeneity prior to the heating at $70^\circ C$ until the clear solution completely transform into milky white gelatin. The gelatin was transferred to a drying oven and kept for 3 days at $110^\circ C$, to remove excess water. The dried sample was crushed in at least 2 hours to obtain homogeneous dispersion of the powder, before being annealed in 4 hours at three different temperatures, $300^\circ C$ and $400^\circ C$, respectively.

3.2.1.2 Sample Characterization

The as-synthesized nanoparticles were characterized by using X-Ray Diffraction (XRD), Field Emission Scanning Electron Microscopy (FESEM) and Energy Dispersive X-ray Spectroscopy (EDX). XRD was used for the identification of phases, crystal structure and determination of crystallite size. To study the morphology of the samples, Field Emission Scanning Electron Microscope (FESEM) was used together with Energy Dispersive X-Ray Spectroscopy (EDX) to determine the chemical composition of the ZnO samples.

3.2.1.3 Preparation of ZnO Nanofluids

ZnO nanofluids were prepared by using two steps method. The nanoparticles were dispersed in deionized water as the base fluid and magnetically stirred in 1 hour duration to produce ZnO nanoparticles suspension. A surfactant, sodium dodecyl sulphate (SDS) 90.0% purity from R&M Chemicals was added into the suspension to improve the stability of the nanofluid. The suspension was then agitated in an ultrasonic cleaner at temperature 25°C for 1 hour to ensure homogeneous dispersion in the base fluid. ZnO nanoparticles have to be dispersed in liquid to enable the Metallic Grid Test to be carried out for cleaning efficiency measurement purposes.

3.2.1 Nano-fluid Preparation Metallic Grid Test.

This test is based on the metallic grid (60 meshes) from the Viscometer Fann 35 SA apparatus to check the nano-spacer cleaning abilities by testing on different type of spacers. The procedure to handle the experiment is as below:

- i. The Fann 35 SA bob is removed.
- ii. Rotor is assembled and grid is immersed into spacer for 10 minutes, then the fluid is dripped off for 2 minutes and spacer excess is removed by wiping using towels.
- iii. Grid is weighted by balance (W4).
- iv. Rotor and grid are washed and dried repeating the passage number 2 with OBM bathing (W2).
- v. Fann beaker is filled up with spacer.
- vi. The grid is rotated at 100 RPM for 5 minutes and then is taken out of the test solution. The rotor is dripped off again for 2 minutes. The rotor bottom is wiped off gently using a paper towel to remove any drops hanging down. It is very important not to remove the mud still adherent on the grid.
- vii. Rotor and grid are taken off and are weighted upside down on balance (W3).
- viii. The passage numbers 6-7 are repeated four times: last time the rotor turned on at 100 RPM for 10 minutes.
- ix. Calculate the percentage of remained mud by using the following formula.

$$\% \text{ Mud Removal} = 100(1-(W3-W4)/(W2-W4))$$

3.2.3 Interfacial Tension Test (IFT) Spinning Drop.

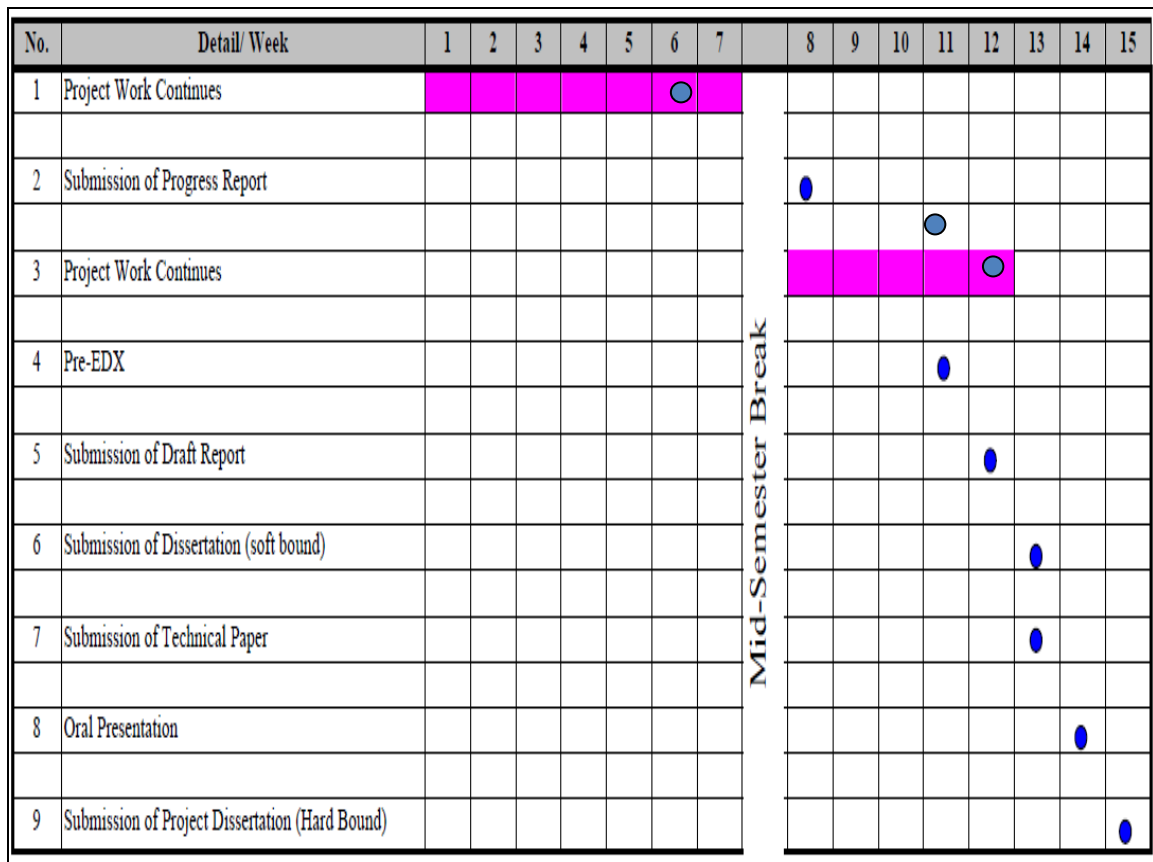
The spinning drop method (rotating drop method) is one of the methods used to measure interfacial tension. Measurements are carried out in a rotating horizontal tube which contains a dense fluid. A drop of a less dense liquid or a gas bubble is placed inside the fluid. Since the rotation of the horizontal tube creates a centrifugal force towards the tube walls, the liquid drop will start to deform into an elongated shape; this elongation stops when the interfacial tension and centrifugal forces are balanced. The surface tension between the two liquids (for bubbles: between the fluid and the gas) can then be derived from the shape of the drop at this equilibrium point. A device used for such measurements is called a “spinning drop tensiometer”.

The purpose of this test is carry out is to check the interfacial tension from the Jatropha oil based mud. Here we will be using a total of 6 samples which are; Brine, SDS only, Nano-fluid in SDS, Nano-fluid in EG solution and 2 of the nano-fluid after aging process. Below is the procedure to check the Inter-Facial tension.

1. Prepare a 100 ml of Brine.
2. Fill in the tube (12.7mm diameter, 165mm long) of the Spinning Drop Tensiometer; SDT.
3. Close it with an end plug and make sure there is no bubble and air is in the tube.
4. Place the tube in the tensiometer and rotate it at a 1000 rpm rate.
5. Create a suspension with a Jatropha Oil Based mud into a syringe a roughly 0.073ml.
6. Insert the suspension into the tube which were placed in the tensiometer earlier.
7. Identify the length of the suspension size.
8. Increase the rpm until the Jatropha Oil Based Mud suspension size were 3 times longer than its original size.
9. Calculate the IFT reading from the software.
10. Repeat step 1 – 8 by using SDS only, Nano-fluid in SDS, Nano-fluid in EG solution and 2 of the nano-fluid after aging process.

3.3 Gantt chart

Below is the Gantt chart for FYP 2.



 Suggested milestone
 Process

TABLE 3B: Gantt chart for FYP2

CHAPTER 4: RESULTS AND DISCUSSION

4.1 Nano-Fluid Preparation.

X-Ray Diffraction Result

X-ray diffraction (XRD) analyses for both samples were performed on all samples using Bruker D8 X-Ray Diffractometer. The analysis was conducted at 25°C, using CuK α radiation of wavelength $\lambda=1.5406\text{\AA}$, operated with scanning angles (2θ) from 10° to 80°, in 0.05° step size.

XRD patterns for ZnO by using Ethylene Glycol is annealed at different temperatures are shown in Figure 8A. All samples are compared with the standard ZnO to see whether there's an exhibit matching pattern. The major diffraction peaks of [100] and [101] suggested that $\langle 100 \rangle$ and $\langle 101 \rangle$ are the favored direction of growth. From the analysis, annealing temperature of 300°C was not sufficient to remove residual water and excess zinc nitrate which was not completely reacted with the solvent during the chemical reaction. However, at temperature 400°C, crystallinity starts improving and impurities starts to disappear and stable hexagonal wurtzite phase begin to form. Moreover, ZnO produced by using Nitric Acid which is annealed at 3 different temperature; 300°C, 400°C and 500°C XRD results is shown in Figure 8B and it also compared with the standard ZnO to check for an exhibit matching pattern.

The crystallite size of the nanoparticle was determined by the means of an X-ray line-broadening method using Scherrer equation;

$$d_{hkl} = \frac{k\lambda}{\beta_{hkl} \cos \theta}$$

Robert M. Beirut. (1976)

(4)

where K is the Scherrer constant, which was chosen to be 0.89 in this analysis, λ is the wavelength of the X-ray used in the diffractometer, B_{hkl} is the peak width at half-maximum intensity and θ is the peak position. Crystallinity and annealing

temperature had contributed to the average crystallite size of the ZnO nanoparticles, whereby size of the crystals were smaller as the annealing temperature increase and material become more orderly arranged. With increasing annealing temperature, the diffraction peaks clearly became narrower, indicating an enhancement of crystallinity.

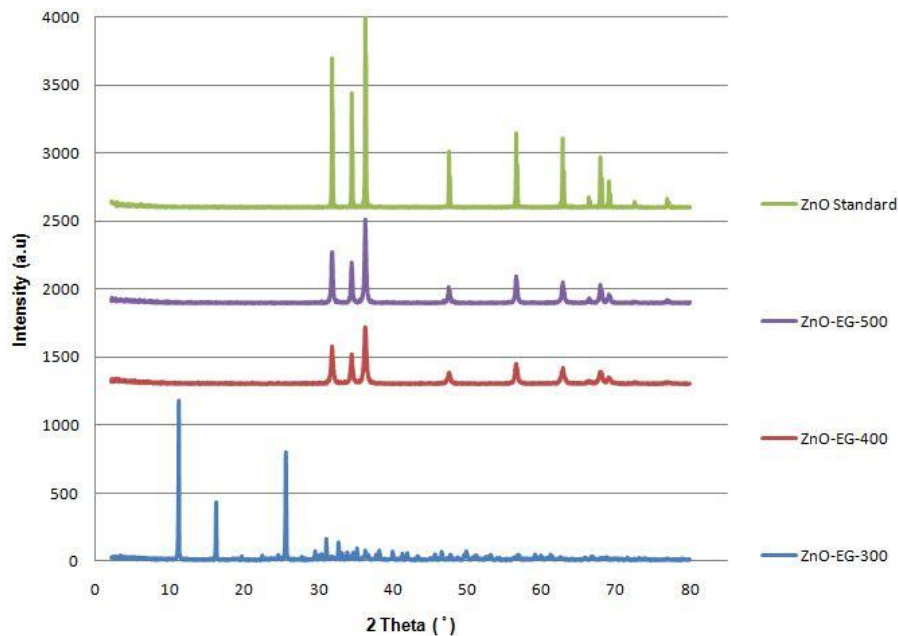


FIGURE 8A: XRD Pattern for ZnO using Ethylene Glycol (EG) nanoparticles for standard ZnO and annealed at temperature 300°C and 400°C

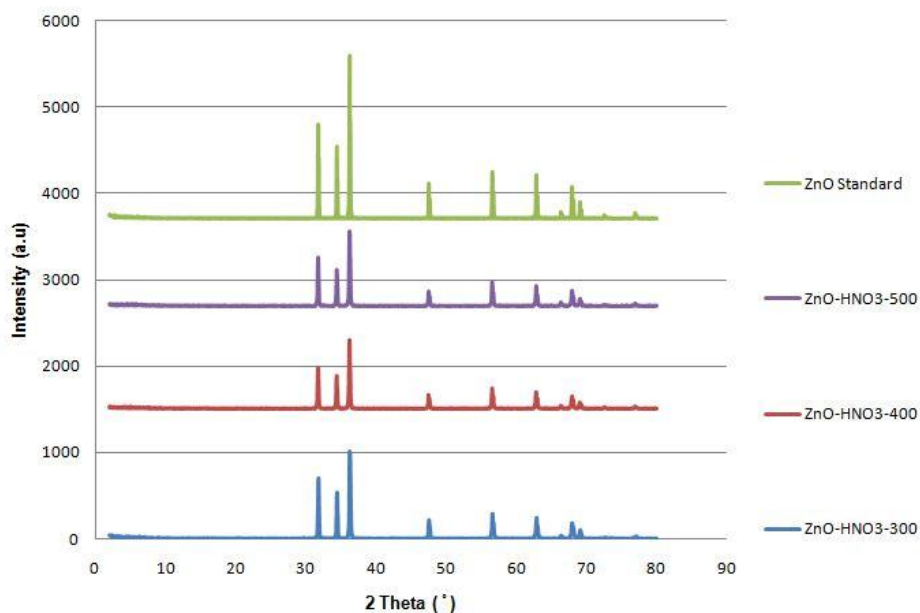


FIGURE 8B: XRD Pattern for ZnO using Nitric Acid (HNO₃) nanoparticles for standard ZnO and annealed at temperature 300°C and 400°C

TABLE 4: Comparative values of crystal planes, d-spacing, lattice parameter, structure and crystallite size of ZnO nanoparticles annealed at various temperatures

XRD Analysis					
Samples	Crystal Planes	d-spacing (Å)	Crystallite Size (nm)	Lattice Parameter	Structure
ZnO-EG 300	(1 0 0)	7.968	133.8	a = 7.038 b = 9.658 c = 11.182 c/a = 1.59	Monoclinic
ZnO-EG 400	(1 0 1)	2.477	27.47	a = 3.2488 b = 3.2488 c = 5.2054 c/a = 1.602	Hexagonal
ZnO-EG 500	(1 0 1)	2.477	52.33	a = 3.2498 b = 3.2498 c = 5.2066 c/a = 1.602	Hexagonal
ZnO-HNO₃ 300	(1 0 1)	2.473	45.93	a = 3.249 b = 3.249 c = 5.205 c/a = 1.60	Hexagonal
ZnO-HNO₃ 400	(1 0 1)	2.475	84.37	a = 3.250 b = 3.250 c = 5.207 c/a = 1.602	Hexagonal
ZnO-HNO₃ 500	(1 0 1)	2.478	96.10	a = 3.249 b = 3.249 c = 5.205 c/a = 1.602	Hexagonal

As summarized in Table 4, it was observed that there was little change in the lattice parameters when the annealing temperature was increased. Changes in the lattice parameter can be affected by free charge, impurities, stress, change of particle size, quantum size effects and temperature [6, 7]. For zinc oxide, the c/a ratio shows variation from 1.593 to 1.6024, which slightly deviates from that of the ideal wurtzite crystal, most probably due to lattice stability and ionicity [7]. However, at some point, when temperature is increase, the ZnO particles tend to coagulate form larger particles.

Field Emission Scanning Electron Microscope (FESEM) Results

FESEM images for ZnO nanoparticles are shown in FIGURE 9 & 10 captured at up to 100,000 times magnification. From the morphology analysis, crystallinity and homogeneity of the nanoparticles began to improve when the annealing temperature increase. As expected, sample annealed at 400°C exhibit sphere-like structure formation and distributed more homogeneously, compared to samples annealed at 300°C. All Zinc Oxide nanoparticles were successfully synthesized by using sol gel method and been treated at temperature of 300°C, 400°C, and 500°C.

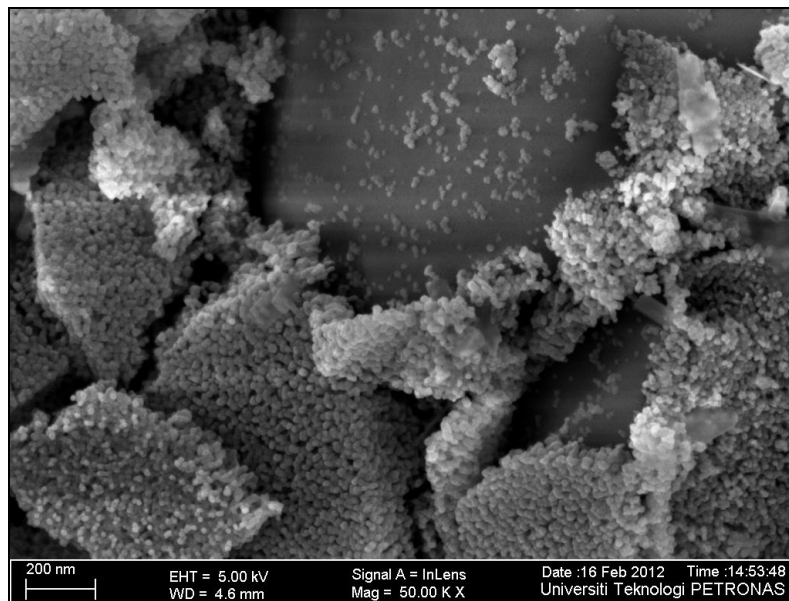


FIGURE 9A: FESEM image For ZnO by using Ethylene Glycol nanoparticles annealed at temperature 300°C

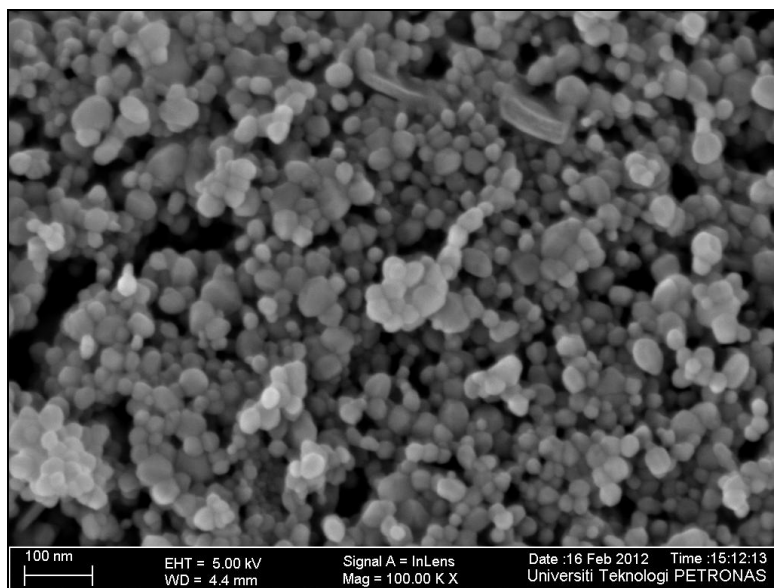


FIGURE 9B: FESEM image For ZnO by using Ethylene Glycol nanoparticles annealed at temperature 400°C

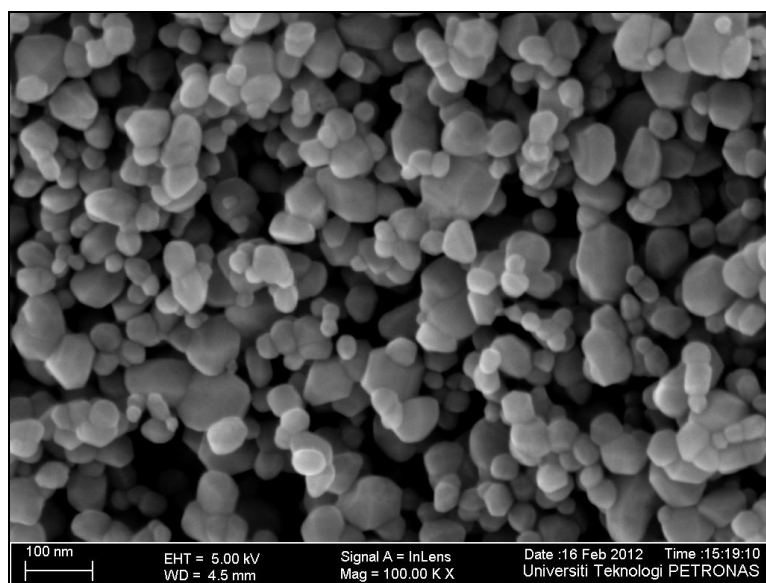


FIGURE 9C: FESEM image For ZnO by using Ethylene Glycol nanoparticles annealed at temperature 500°C

Not to forget, Zinc Oxide is also successfully obtained by using Nitric Acid via sol gel method and heat treatment at temperatures 300°C, 400°C, and 500°C. Figure 6A, 6B and 6C shows the Field Emission Scanning Electron Microscope (FESEM) images for all three samples captured at 10,000 times magnification. As shown in all the figures, all samples exhibits rod-like structures formation and distributed more homogeneously.

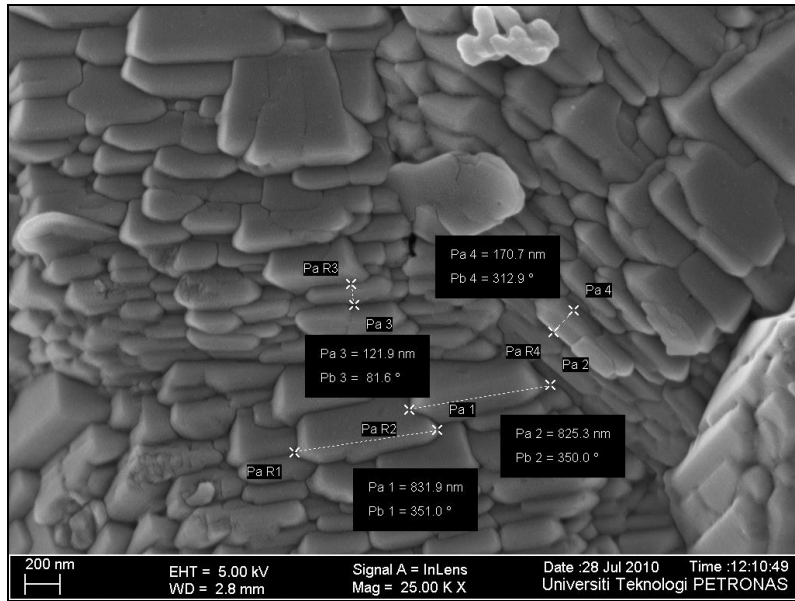


FIGURE 10A: FESEM image For ZnO by using Nitric Acid nanoparticles annealed at temperature 300°C

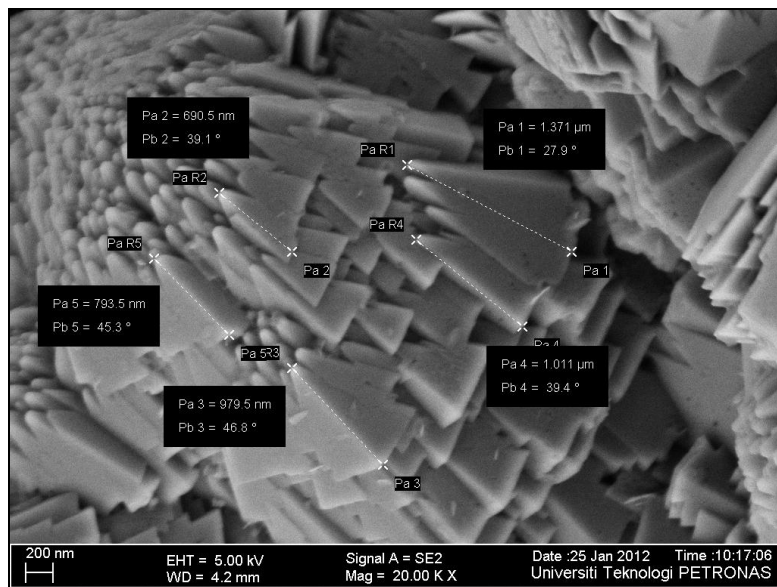


FIGURE 10B: FESEM image For ZnO by using Nitric Acid nanoparticles annealed at temperature 400°C

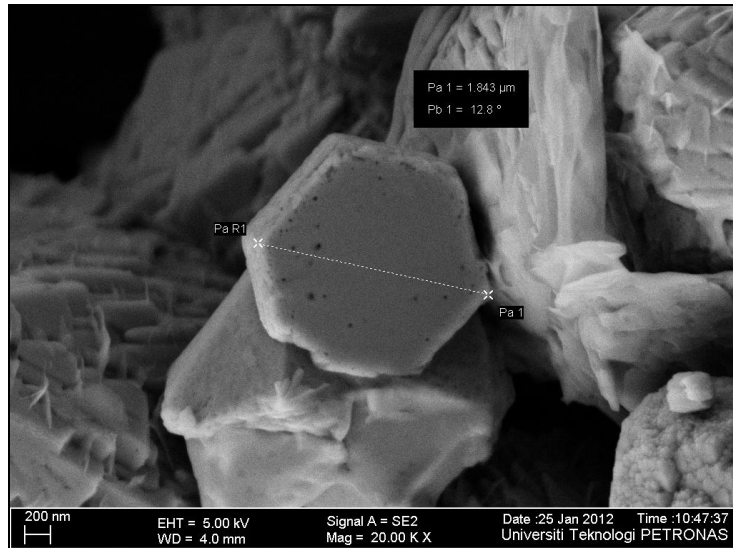


FIGURE 10C: FESEM image For ZnO by using Nitric Acid nanoparticles annealed at temperature 500°C

Energy Dispersive X-Ray (EDX) Result

Elemental composition of the sample can be identified from EDX analysis by using OXFORD INCA X-ray Microanalysis system. The atomic and weight percentages of these elements together with the deviation analysis can be obtain and Table 2 is the summary of the results obtained. From the EDX analysis, presence of Zinc (Zn) and Oxygen (O) are evident by the relative abundance of each of the element which is comparable to the theoretical stoichiometric values. It can be concluded that ZnO nanoparticles produced were of high purity, with the presence of no element other than Zn and O in the compound. The ratio of the Zn:O atoms should 1:1 or 50-50 based on the chemical formula; ZnO. However there's a little deviation in the atomic percentage was observed. Standard atomic weight of oxygen atom is 15.9994g/mol and 65.38g/mol for zinc. From this EDX analysis, there is a huge deviation in weight percentage for zinc oxide samples sintered at 300 °C for sample made of Ethylene Glycol, however smaller deviation was observed for other samples as this is due to the annealing temperature is sufficient to remove the residual water and impurities.

Sample	Elements	Weight (%)	Atomic (%)
ZnO-EG 300 °C	O	44.30	76.47
	Zn	55.70	23.53
ZnO-EG 400 °C	O	24.96	57.62
	Zn	75.04	42.38
ZnO-EG 500 °C	O	21.25	52.44
	Zn	78.75	47.56
ZnO-HNO ₃ 300 °C	O	20.36	20.36
	Zn	79.64	79.64
ZnO-HNO ₃ 400 °C	O	19.55	49.82
	Zn	80.45	50.18
ZnO-HNO ₃ 500 °C	O	17.58	46.56
	Zn	82.42	53.44

TABLE 5: Elemental distribution analysis of zinc oxide nanoparticles annealed at various temperatures.

In conclusion, based on the methodology to obtain the nano particles of Zinc Oxide, we have picked the sample ZnO -EG-400 °C. This is because of the particle made from mixing Zinc Nitrate with Ethylene Glycol and continuous stirring time up to 14 days has the ability to produce an average 27 nm crystallite sizes after annealed at temperature 400 °C. This sample was then used for further research in metallic grid test and IFT test.

4.2 Metallic Grid Test

	Time (mins)	SDS only (g)	%Mud Removal	Nano-fluid (ZnO 1wt% + SDS 0.3wt%)	%Mud Removal	Nano-fluid (after aging process) (ZnO 1wt% + SDS 0.3wt%)	%Mud Removal
Clean with spacer (W4)		140.414		140.603		140.563	
Weight with OBM bath (W2)		141.623		141.898		142.271	
Clean with spacer; 100 RPM (5 minutes)	5	141.612	0.910	141.574	25.019	141.781	28.689
Clean with spacer; 100 RPM (10 minutes)	10	141.424	16.460	141.383	39.768	141.623	37.939
Clean with spacer; 100 RPM (15 minutes)	15	141.286	27.874	141.201	53.822	141.463	47.307
Clean with spacer; 100 RPM (20 minutes)	20	141.183	36.394	141.065	64.324	141.298	56.967
Clean with spacer; 100 RPM (30 minutes)	30	140.979	53.267	141.007	68.803	141.181	63.817

TABLE 6A: Table Results for Metallic Grid Test

	Time (mins)	Nano-fluid in 60% EG solution (ZnO 1wt%)	%Mud Removal	Nano-fluid in 60% EG solution(after aging process) (ZnO 1wt%)	%Mud Removal	Conventional Spacer A (Without Baryte)	%Mud Removal	Conventional Spacer B (Without Baryte)	%Mud Removal
Clean with spacer (W4)		140.673		140.563		140.586		140.579	
Weight with OBM bath (W2)		141.848		141.981		141.864		141.964	
Clean with spacer; 100 RPM (5 minutes)	5	141.497	29.872	141.652	23.202	141.791	5.712	141.678	20.650
Clean with spacer; 100 RPM (10 minutes)	10	141.247	51.149	141.428	38.999	141.701	12.754	141.543	30.397
Clean with spacer; 100 RPM (15 minutes)	15	141.084	65.021	141.202	54.937	141.638	17.684	141.479	35.018
Clean with spacer; 100 RPM (20 minutes)	20	141.053	67.660	141.104	61.848	141.599	20.736	141.409	40.072
Clean with spacer; 100 RPM (30 minutes)	30	141.018	70.638	141.073	64.034	141.589	21.518	141.348	44.477

TABLE 6B: Table Results for Metallic Grid Test

According to TABLE 6A and TABLE 6B of the metallic grid test carried out by using the nano fluid produced by sol gel method. During this experiment, an oil based mud from Jatropa Oil is used. Below are the properties of OBM used for this experiment.

Based Oil:	Jatropa Oil
Mud Weight:	13 ppg
Ø600: 73	Ø300: 40
Ø200: 27	Ø100: 16
Plastic Viscosity: 33	Yield Point: 7
Gel Strength 10 sec: 9	Gel Strength 10 min: 11

Its shows that by using the nano fluid we can obtain a cleaning efficiency up to 70%. In order to compare, a base fluid of deionised water mixed with SDS is also tested. Referring to Figure 11A, we can obtain the increment of cleaning efficiency by using the ZnO nanoparticles into the aqueous solution. The function of SDS in this experiment is to stabilized the nano fluid suspension and improve the dispersion of the material inside the aqueous solutions. For comparison purposes, we also have suspend the ZnO into a 60% Ethylene Glycol and 40% Deionised water solution to prove that the ZnO nanoparticles is the reason why the cleaning efficiency is improved.

Comparison with the conventional spacer used in oil and gas industry is also made. The maximum cleaning that can be achieved by using conventional spacer is only up to 45%. Moreover, all samples has gone through an aging process where hot rolling treatment of 100 °C and 50psia is applied for 16 hours to all sample and the cleaning efficiency is not affected. Thus by adding only 1 wt% of the nano particles we can obtain an increment of 25% thus improve the cleaning of the wellbore casing for promoting better cement bonding during cementing operations.

Figure 11A, 11B and 11C shown the line graphs for a clearer picture to show that small amount of ZnO (1 wt%) are able to improve the cleaning efficiency of spacer during cementing operation.

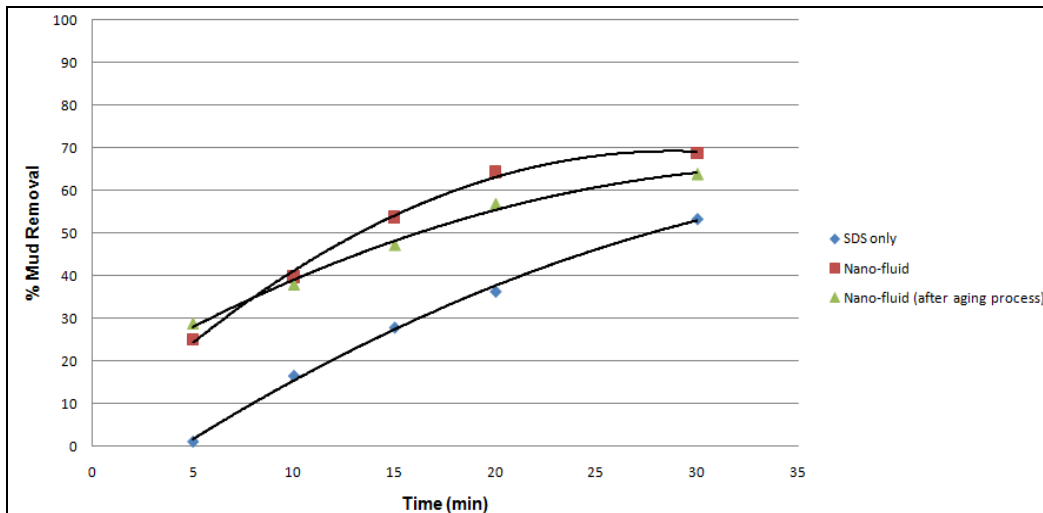


FIGURE 11A: Graph for Nano-fluid Metallic Grid Test.

Based on the Figure 11A, we can obtain the graphical results of using nano-fluid (1wt% ZnO and 0.3wt% SDS) and also after aging at 110°C for 16 hours through hot rolling. We can obtain that, as early as 5 minutes, more than 20% of mud is able to be removed in such a short period if we were to compare with an aqueous solution which only contains SDS only. While a maximum of up to 70% mud removal can be obtained after the experiment is carried out after 30 minutes. It shows that the existence of nano-particles has a significant effective result in cleaning efficiency compared to an aqueous solution which does not contain the nanoparticles.

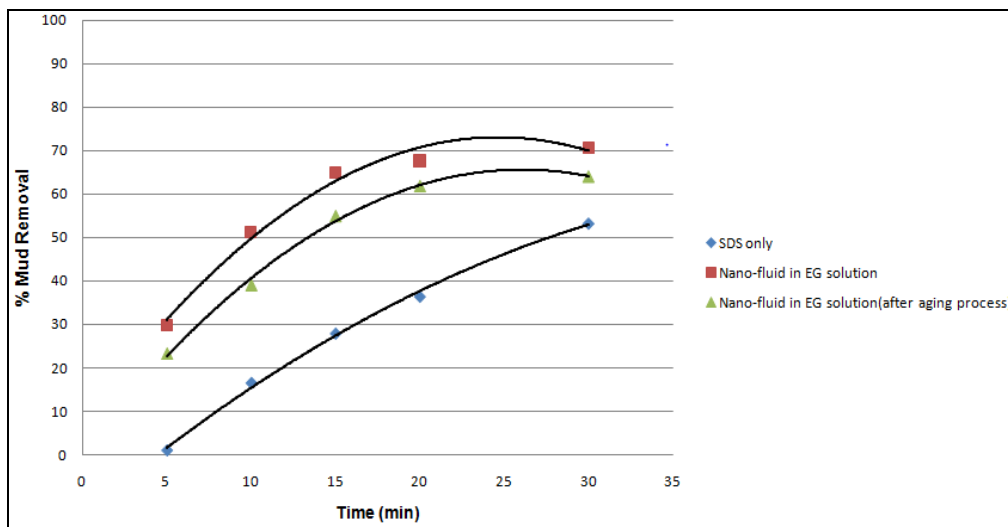


FIGURE 11B: Graph for Nano-fluid by using Ethylene Glycol as a dispersed medium Metallic Grid Test.

Based on the Figure 11B, we can obtain the graphical results of using nano-fluid (1wt% ZnO in 60% Ethylene Glycol solution) and also after aging at 110°C for 16 hours

through hot rolling. We can obtain that, as early as 5 minutes, more than 25% of mud is able to be removed in such a short period if we were to compare with an aqueous solution with only contains SDS only. While a maximum of up to 70% mud removal can be obtain after the experiment is carry out after 30 minutes. It shows that the existence of nano-particles in a solution have the ability to effectively cleans the wellbore compared to an aqueous solution which does not contain the nanoparticles.

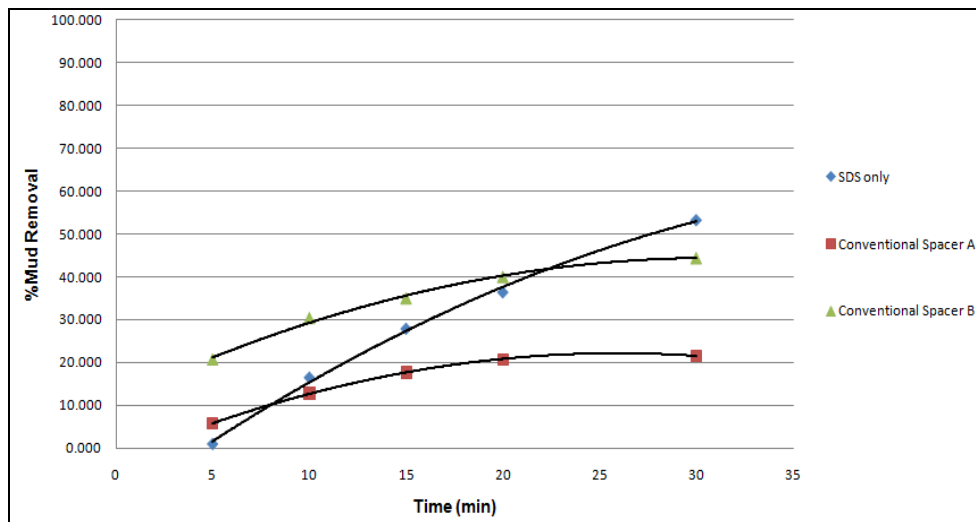


FIGURE 11C: Graph for Conventional Spacer Metallic Grid Test.

Based on Figure 11C, we can obtain the metallic grid test result by using the conventional mixture for spacer use during operation in offshore. We can obtain that at 5 minutes, for conventional A shows a cleaning efficiency less than 10% mud removal, thus making it unsuitable for effective cleaning to promote cement bonding while conventional spacer B shows a better results where more than 20% mud removal can be obtain in just 5 minutes. However, at 30 minutes, conventional spacer A only show a maximum mud removal of 20% while conventional spacer B only records a maximum % of mud removal of up to 45% only.

If we compare to the metallic grid test result for the aqueous solution with nano-particles in it, a maximum of 70% mud removal is obtained thus making nano-spacer a better cleaning agent to be used during operation in during drilling and completion.

4.3 Interfacial Tension Test (IFT).

Sample (Phase 1)	Sample (Phase 2)	IFT (mN/m)
Brine; Distilled Water + CaCl ₂	Jatropha Oil Based Mud	15.487
SDS only; 0.3 wt%	Jatropha Oil Based Mud	1.357
Nano-fluid; ZnO 1.0 wt % + SDS 0.3 wt%	Jatropha Oil Based Mud	2.203
Nano-fluid; ZnO 1.0 wt % + SDS 0.3 wt% (After aging)	Jatropha Oil Based Mud	2.319
Nano-fluid in 60% EG solution; ZnO 1.0 wt%	Jatropha Oil Based Mud	2.562
Nano-fluid in 60% EG solution; ZnO 1.0 wt% (After aging)	Jatropha Oil Based Mud	2.897

Table 7: Table Results for Contact Angle Test

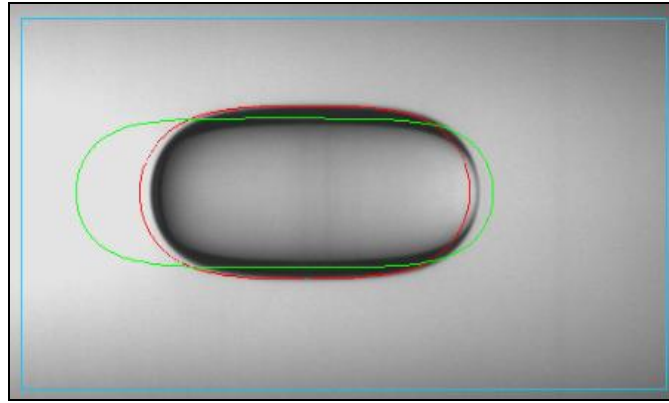


FIGURE 12A: Snapshot image from SVT20 Tensiometer during the measurement shows the drop size at rotation 1,000 rpm

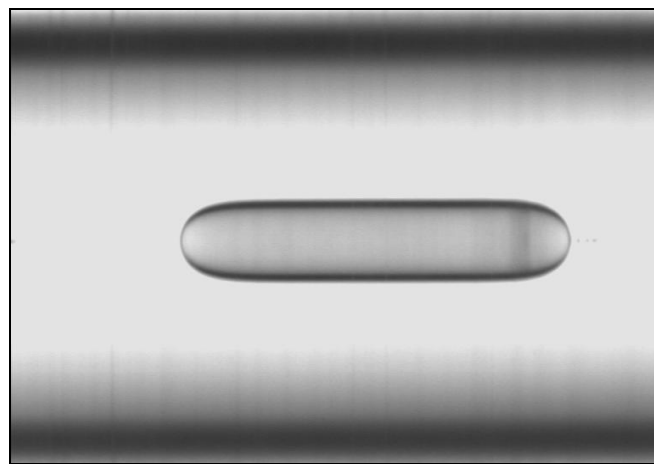


FIGURE 12B: Snapshot image from SVT20 Tensiometer during the measurement shows the drop size at rotation 5,000 rpm

Based on the table above, we can obtain the results for the IFT test via spinning drop tensiometer methods. This equipment has the ability to identify the desired liquid for interfacial tension reading at different RPM and different at desired temperature.

Initially, Jatropa oil based mud - brine IFT value was measured as 15.847 mN/m, almost in the range of typical OBM - brine IFT, which is around 15-50 mN/m. When 0.3 wt% of aqueous SDS solution is in contact with the crude oil, the IFT value was tremendously decreased to 1.357 mN/m. When SDS molecules are adsorbed at the interface, their hydrophobic tails will reside on the non-polar phase, and their hydrophilic head preferentially orientated towards the aqueous solution, leading to tremendous reduction in interfacial tension [8].

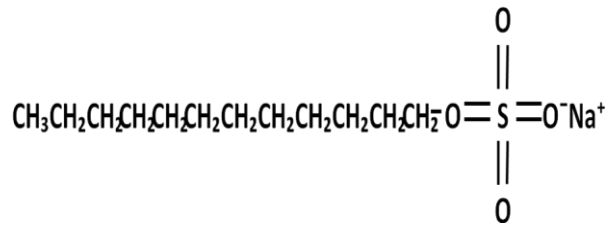


FIGURE 13: Molecular structure of sodium dodecyl sulfate, showing the polar head and non-polar tail [9] (Ref: P. Mukerjee "Critical Micelle Concentration of Aqueous Surfactant Systems")

When the same aqueous SDS solution was used as the base fluid for the nanoparticles suspensions, the IFT values slightly increases as compared to that of the base fluid itself. In mixed systems, the more rapidly adsorbing surfactant was originally located at the interface, and gradually, particles will be irreversibly adsorbed at the interface to replace surfactant molecules, leading to an increase in surface tension. Once at the interface, a particle can be thought of as irreversibly absorbed, behavior unlike surfactants, which are generally thought to be in a state of dynamic equilibrium, absorbing and desorbing on a fast timescale [10]. Another factor which contributes to the increase in IFT values is the particles size. Kinetic study of CdSe nanoparticles on oil-water interface conducted by S. Kutuzov et al. shows that when nanoparticles size decreases, the rate of adsorption of the nanoparticles will subsequently decreases, which explains the lower IFT value observed in ZnO nano-fluids[11].

CHAPTER 5: CONCLUSION AND RECOMMENDATION

5.1 Conclusion

By using the sol gel method, we can obtain the nanoparticles from the steps shown above. Stable, single phase hexagonal wurtzite ZnO is successfully formed at temperature of 400 °C for samples which are formed by using Ethylene Glycol and at 300 °C for ZnO sample formed by using Nitric Acid. The main purpose of using two (2) different solvent is to find out which solvent will produce a sphere shape of nanoparticles of zinc oxide with the smallest crystallite size . By using Ethylene Glycol and heat treatment at 400 °C gives an average crystallite size of 27nm. Thus this sample; Zinc Oxide by using Ethylene Glycol with heat treatment at 400 °C (ZnO-EG-400) is used for further experiment in searching alternative to replace the conventional spacer.

Next, the ZnO is successfully dispersed in water by using deionised water and also sodium dodecyl sulphate to help the nano particles to be dispersed inside the aqueous solution. In metallic grid test, by using the ZnO nanoparticles dispersed in an aqueous solution shows an increased of cleaning efficiency compared to the conventional spacer. It also proved that the nano fluid shows a reduction of interfacial tension of the oil based mud by using the spinning drop tensiometer equipment.

5.2 Recommendations

For further research in nano-spacer technology, studies about the dielectric properties of Zinc Oxide should be carry out. This is called as electrorheology (ER) theory. According to the theory, nano-materials metal oxides has the ability to act as a transistor which could alters and increases the rheology of the nano-fluid after subjected to an electromagnetic field. With that, it can improve the cleaning efficiency of the nano-spacer. Not to forget, when electromagnetic is emitted, we can alter the rheology in terms of viscosity. Thus, with it we can reduce cost in using nanoparticles instead of Viscosifier polymers.

REFERENCES

1. Sarap, Sivanandan, Patil, Deshpande. (2009): “The Use of High-Performance Spacer for Zonal Isolation in High Temperature High Pressure Wells”, paper SPE/IADC 124275 presented at Annual SPE/IADC Middle East Drilling Technology Conference & Exhibition held in Manama, Bahrain, 26-28 October 2009, pp1-7.
2. Maserati, Daturi (2010): “Nano-Emulsion as Cement Spacer Improve the Cleaning of Casing Bore during Cementing Operations”, paper SPE 133033 presented at Annual SPE Technical Conference and Exhibition held in Florence, Italy, 19-22 September 2010, pp1-10.
3. Ryan van Zanten, Bridget Lawrence, Stephen Henzler. (2010): “Using Surfactant Nanotechnology to Engineer Displacement Packages for Cementing Operations”, paper IADC/SPE 127885 presented at Annual IADC/SPE Drilling Conference and Exhibition held in New Orleans, Louisiana, USA, 2-4 February 2010, pp1-6.
4. Robert M. Beirut. (1976): “All Purpose Cement-Mud Spacer”, paper SPE 5691 presented at AIME Symposium on Formation Damage Control held in Houston, Texas, 29-30 January 1976, pp1-8.
5. Lawrence Webber. (2004), “Global Best Practice for Cementing”, UNOCAL Corporation Central Drilling Group.
6. A Khorsand Zak et.al, Effects Of Annealing Temperature On Some Structural And Optical Properties Of ZnO Nanoparticles Prepared By A Modified Sol-Gel Combustion Method, *Ceramics International*, vol.37, pp. 393-398, 2011.
7. H. Morkoç and Ü. Özgür, *Zinc Oxide: Fundamentals, Materials and Device Technology*, Wiley-VCH Verlag GmbH & Co., 2009.
8. H. B. de Aguiar et. al, The Interfacial Tension of Nanoscopic Oil Droplets in Water Is Hardly Affected by SDS Surfactant, *J. Am. Chem. Soc.*, vol. 132, pp. 2122–2123, 2010.
9. J.L. Salager, *Interfacial Phenomena in Dispersed Systems*, FIRP Booklet # 120-N, 1994.

10. T.N. Hunter et al. / *Advances in Colloid and Interface Science* 137, 57–81, 2008.
11. S. Kutuzov et. al, On the kinetics of nanoparticle self-assembly at liquid/liquid interfaces *Phys. Chem. Chem. Phys.*, 9, 6351–6358, 2007.

APPENDICES

Spectrum processing:

Peak possibly omitted: 0.262 keV

Processing option : All elements analyzed (Normalised)

Number of iterations = 3

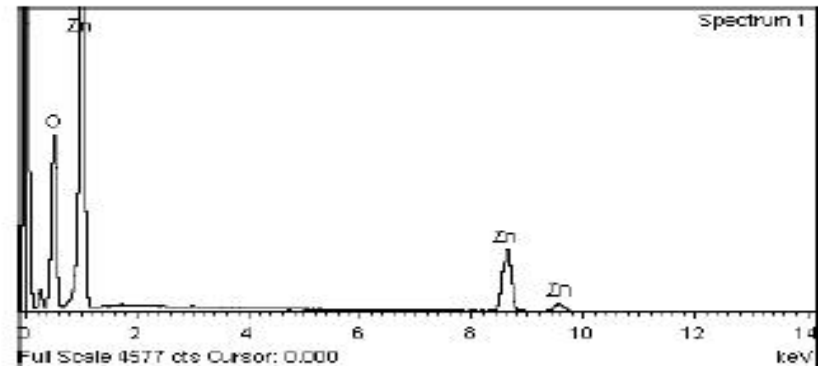
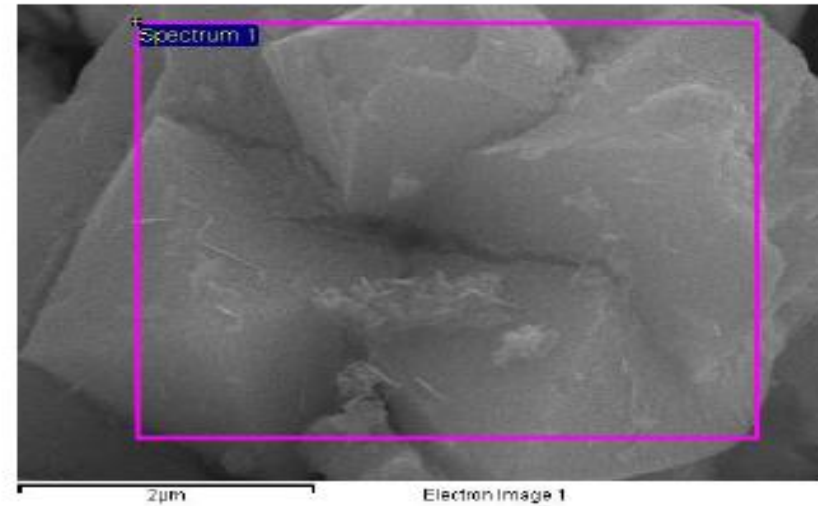
Standard:

O SiO2 1-Jun-1999 12:00 AM

Zn Zn 1-Jun-1999 12:00 AM

Element	Weight%	Atomic%
O K	44.30	76.47
Zn K	55.70	23.53
Totals	100.00	

Comment:



Spectrum processing :

No peaks omitted

Processing option : All elements analyzed (Normalised)

Number of iterations = 2

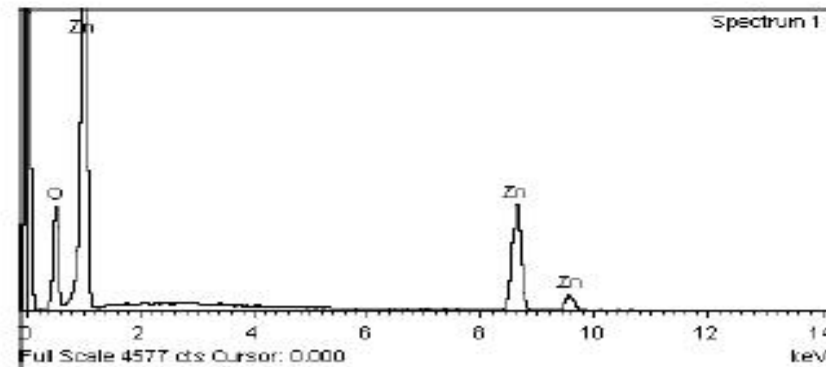
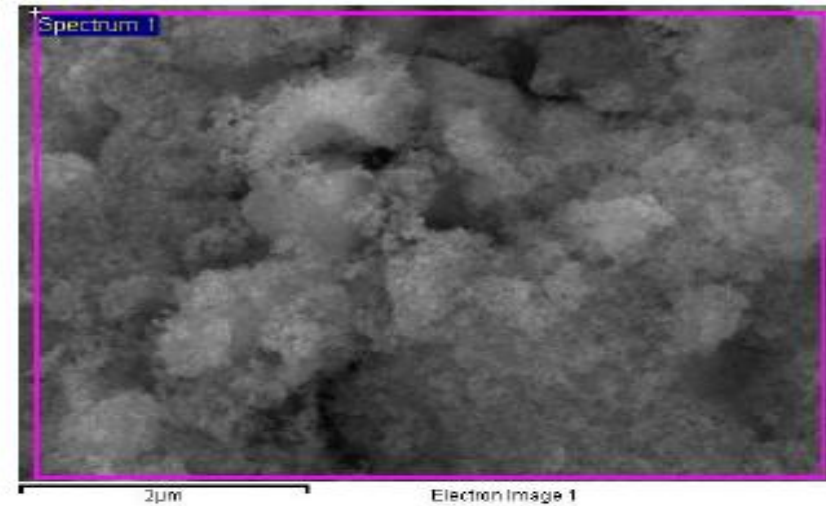
Standard :

O SiO2 1-Jun-1999 12:00 AM

Zn Zn 1-Jun-1999 12:00 AM

Element	Weight%	Atomic%
O K	24.96	57.62
Zn K	75.04	42.38
Totals	100.00	

Comment:



Spectrum processing :

Peaks possibly omitted : 0.260, 11.040 keV

Processing option : All elements analyzed (Normalised)

Number of iterations = 3

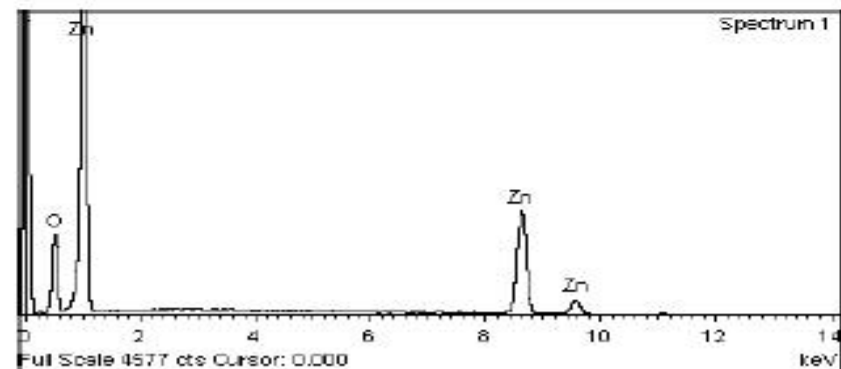
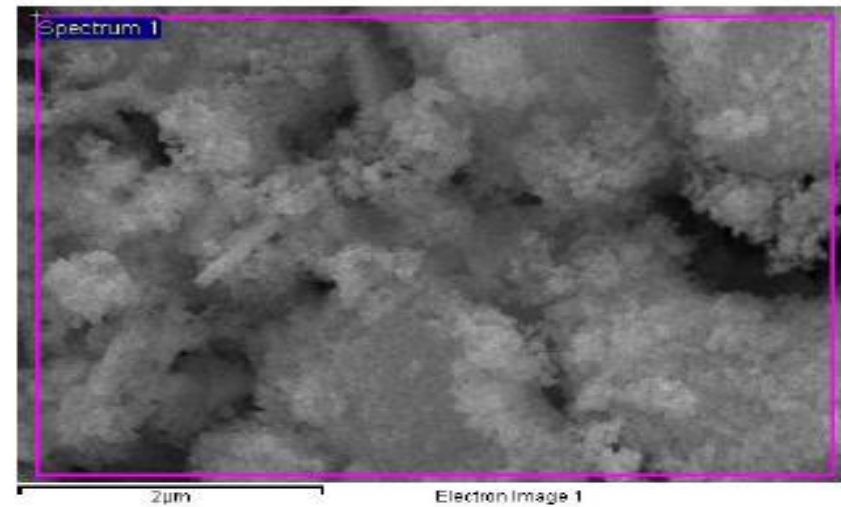
Standard :

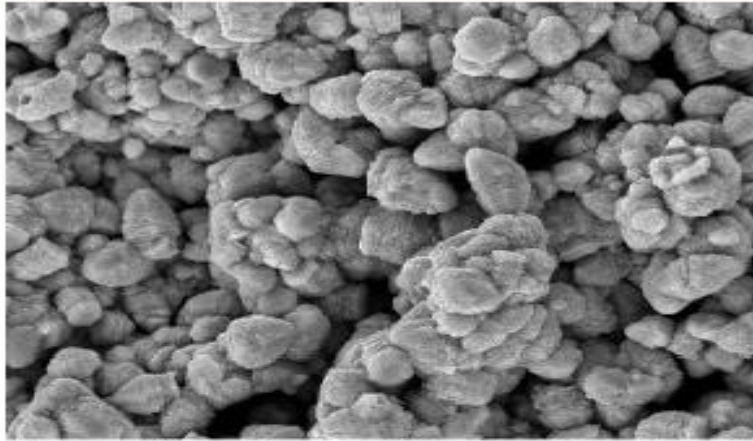
O SiO2 1-Jun-1999 12:00 AM

Zn Zn 1-Jun-1999 12:00 AM

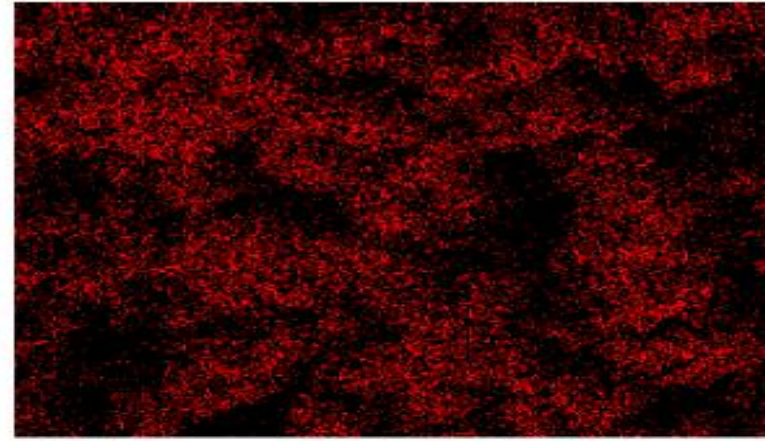
Element	Weight%	Atomic%
O K	21.25	52.44
Zn K	78.75	47.56
Totals	100.00	

Comment:

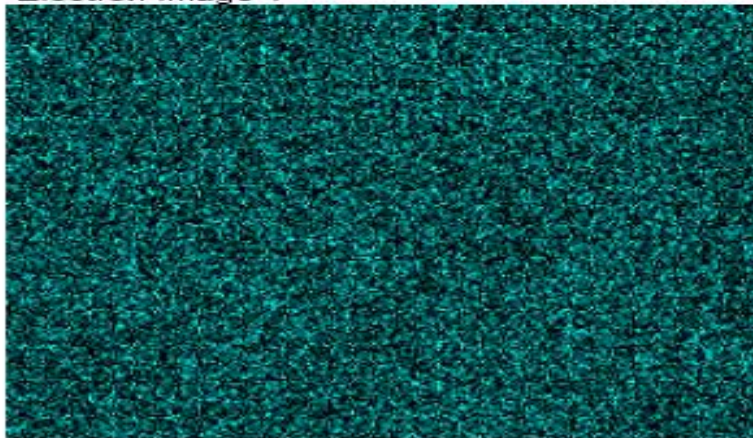




Electron Image 1



O Ka1



Zn Ka1

Spectrum processing :

No peaks omitted

Processing option : All elements analyzed (Normalised)

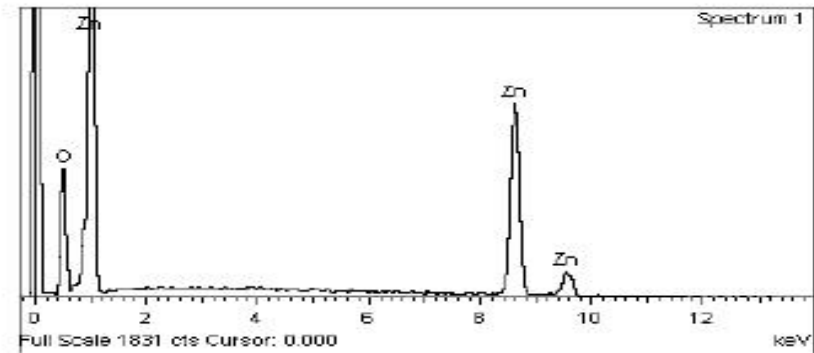
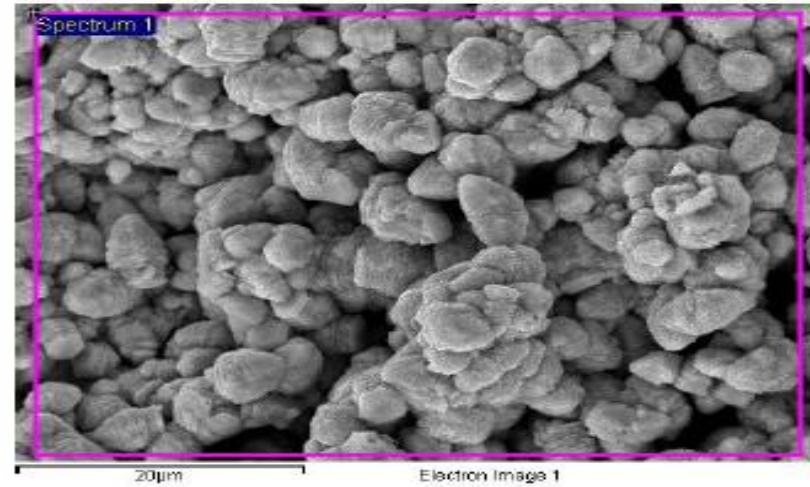
Number of iterations = 3

Standard :

O SiO₂ 1-Jun-1999 12:00 AM

Zn Zn 1-Jun-1999 12:00 AM

Element	Weight%	Atomic%
O K	19.55	49.82
Zn K	80.45	50.18
Totals	100.00	



Comment:



Spectrum processing :

No peaks omitted

Processing option : All elements analyzed (Normalised)

Number of iterations = 3

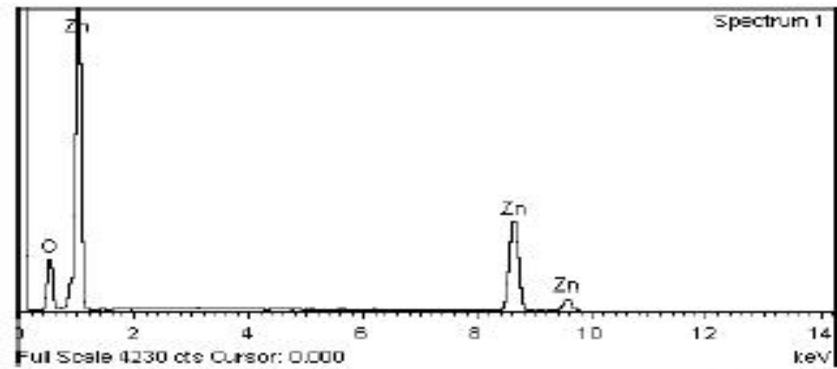
Standard :

O SiO₂ 1-Jun-1999 12:00 AM

Zn Zn 1-Jun-1999 12:00 AM

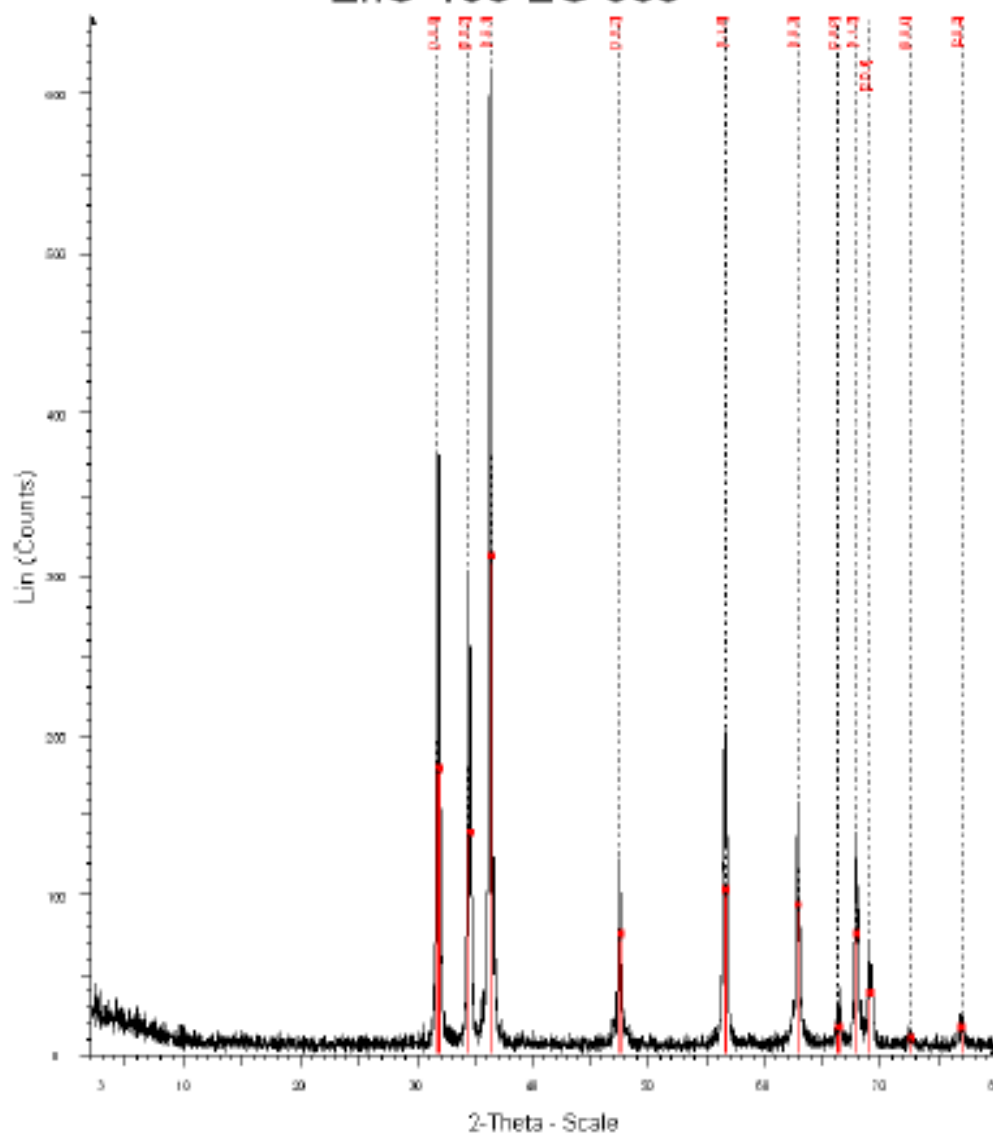
Element	Weight%	Atomic%
O K	17.58	46.56
Zn K	82.42	53.44
Totals	100.00	

Comment:



XRD Results for ZnO-EG-500

ZnO-100-EG 500



ZnO-100-EG 500 - File: ZnO-100-EG 500.xrd - Type: 2 θ RT - Index - Start: 2.800 ° - End: 80.000 ° - Step: 0.020 ° - Step time: 1 s - Temp.: 25 ° C
Operator: isport

00-1451 () - ZnO (R) - ZnO - Y: 90.00% - IC: 01 - WL: 1.5406 - hkl: 010 - 0.524982 - 0.524982 - 0.528951 - 2 θ : 290.000 - 040 90.000 -

XRD Results for ZnO-HNO₃-500

